

91. Axions and Other Similar Particles

Revised October 2019 by A. Ringwald (DESY, Hamburg), L.J. Rosenberg (U. Washington) and G. Rybka (U. Washington).

91.1 Introduction

In this section, we list coupling-strength and mass limits for light neutral scalar or pseudoscalar bosons that couple weakly to normal matter and radiation. Such bosons may arise from the spontaneous breaking of a global U(1) symmetry, resulting in a massless Nambu-Goldstone (NG) boson. If there is a small explicit symmetry breaking, either already in the Lagrangian or due to quantum effects such as anomalies, the boson acquires a mass and is called a pseudo-NG boson. Typical examples are axions (A^0) [1–4] and majorons [5], associated, respectively, with a spontaneously broken Peccei-Quinn and lepton-number symmetry.

A common feature of these light bosons ϕ is that their coupling to Standard-Model particles is suppressed by the energy scale that characterizes the symmetry breaking, *i.e.*, the decay constant f . The interaction Lagrangian is

$$\mathcal{L} = f^{-1} J^\mu \partial_\mu \phi, \quad (91.1)$$

where J^μ is the Noether current of the spontaneously broken global symmetry. If f is very large, these new particles interact very weakly. Detecting them would provide a window to physics far beyond what can be probed at accelerators.

Axions are of particular interest because the Peccei-Quinn (PQ) mechanism remains perhaps the most credible scheme to preserve CP-symmetry in QCD. Moreover, the cold dark matter (CDM) of the universe may well consist of axions and they are searched for in dedicated experiments with a realistic chance of discovery.

Originally it was assumed that the PQ scale f_A was related to the electroweak symmetry-breaking scale $v_{EW} = (\sqrt{2}G_F)^{-1/2} = 247$ GeV. However, the associated “standard” and “variant” axions were quickly excluded—we refer to the Listings for detailed limits. Here we focus on “invisible axions” with $f_A \gg v_{EW}$ as the main possibility.

Axions have a characteristic two-photon vertex, inherited from their mixing with π^0 and η . This coupling allows for the main search strategy based on axion-photon conversion in external magnetic fields [6], an effect that also can be of astrophysical interest. While for axions the product “ $A\gamma$ interaction strength \times mass” is essentially fixed by the corresponding π^0 properties, one may consider a more general class of axion-like particles (ALPs) where the two parameters (coupling and mass) are independent. A number of experiments explore this more general parameter space. ALPs populating the latter are predicted to arise generically, in addition to the axion, in low-energy effective field theories emerging from string theory [7–14]. The latter often contain also very light Abelian vector bosons under which the Standard-Model particles are not charged: so-called hidden-sector photons, dark photons or paraphotons. They share a number of phenomenological features with the axion and ALPs, notably the possibility of hidden photon to photon conversion. Their physics cases and the current constraints are compiled in Refs. [15–17].

91.2 Theory

91.2.1 Peccei-Quinn mechanism and axions

The QCD Lagrangian includes a CP-violating term $\mathcal{L}_\Theta = -\bar{\Theta} (\alpha_s/8\pi) G^{\mu\nu a} \tilde{G}_{\mu\nu}^a$, where $-\pi \leq \bar{\Theta} \leq +\pi$ is the effective Θ parameter after diagonalizing quark masses, $G_{\mu\nu}^a$ is the color field strength tensor, and $\tilde{G}^{a,\mu\nu} \equiv \epsilon^{\mu\nu\lambda\rho} G_{\lambda\rho}^a/2$, with $\epsilon^{0123} = 1$, its dual. Limits on the neutron electric dipole moment [18] imply $|\bar{\Theta}| \lesssim 10^{-10}$ even though $\bar{\Theta} = \mathcal{O}(1)$ is otherwise completely satisfactory. The

spontaneously broken global Peccei-Quinn symmetry $U(1)_{\text{PQ}}$ was introduced to solve this “strong CP problem” [1, 2], the axion being the pseudo-NG boson of $U(1)_{\text{PQ}}$ [3, 4]. This symmetry is broken due to the axion’s anomalous triangle coupling to gluons,

$$\mathcal{L} = \left(\frac{\phi_A}{f_A} - \bar{\Theta} \right) \frac{\alpha_s}{8\pi} G^{\mu\nu a} \tilde{G}_{\mu\nu}^a, \quad (91.2)$$

where ϕ_A is the axion field and f_A the axion decay constant. Color anomaly factors have been absorbed in the normalization of f_A which is defined by this Lagrangian. Thus normalized, f_A is the quantity that enters all low-energy phenomena [19]. Non-perturbative topological fluctuations of the gluon fields in QCD induce a potential for ϕ_A whose minimum is at $\phi_A = \bar{\Theta} f_A$, thereby canceling the $\bar{\Theta}$ term in the QCD Lagrangian and thus restoring CP symmetry.

The resulting axion mass, in units of the PQ scale f_A , is identical to the square root of the topological susceptibility in QCD, $m_A f_A = \sqrt{\chi}$. The latter can be evaluated further [20, 21], exploiting the chiral limit (masses of up and down quarks much smaller than the scale of QCD), yielding $m_A f_A = \sqrt{\chi} \approx f_\pi m_\pi$, where $m_\pi = 135$ MeV and $f_\pi \approx 92$ MeV. In more detail one finds, to next-to-next-to-leading order in chiral perturbation theory [22],

$$m_A = 5.691(51) \left(\frac{10^9 \text{ GeV}}{f_A} \right) \text{meV}. \quad (91.3)$$

A direct calculation of the topological susceptibility via QCD lattice simulations finds almost the same central value, albeit with an about five times larger error bar [23].

Axions with $f_A \gg v_{\text{EW}}$ evade all current experimental limits. One generic class of models invokes “hadronic axions” where new heavy quarks carry $U(1)_{\text{PQ}}$ charges, leaving ordinary quarks and leptons without tree-level axion couplings. The archetype is the KSVZ model [24], where in addition the heavy new quarks are electrically neutral. Another generic class requires at least two Higgs doublets and ordinary quarks and leptons carry PQ charges, the archetype being the DFSZ model [25]. All of these models contain at least one electroweak singlet scalar that acquires a vacuum expectation value and thereby breaks the PQ symmetry. The KSVZ and DFSZ models are frequently used as benchmark examples, but other models exist where both heavy quarks and Higgs doublets carry PQ charges. In supersymmetric models, the axion is part of a supermultiplet and thus inevitably accompanied by a spin-0 saxion and a spin-1 axino, which both also have couplings suppressed by f_A and are expected to have large masses due to supersymmetry breaking [26].

91.2.2 Model-dependent axion couplings

Although the generic axion interactions scale approximately with f_π/f_A from the corresponding π^0 couplings, there are non-negligible model-dependent factors and uncertainties. The axion’s two-photon interaction plays a key role for many searches,

$$\mathcal{L}_{A\gamma\gamma} = -\frac{g_{A\gamma\gamma}}{4} F_{\mu\nu} \tilde{F}^{\mu\nu} \phi_A = g_{A\gamma\gamma} \mathbf{E} \cdot \mathbf{B} \phi_A, \quad (91.4)$$

where F is the electromagnetic field-strength tensor and $\tilde{F}^{\mu\nu} \equiv \epsilon^{\mu\nu\lambda\rho} F_{\lambda\rho}/2$, with $\epsilon^{0123} = 1$, its dual. The coupling constant is [27]

$$g_{A\gamma\gamma} = \frac{\alpha}{2\pi f_A} \left(\frac{E}{N} - 1.92(4) \right) = \left(0.203(3) \frac{E}{N} - 0.39(1) \right) \frac{m_A}{\text{GeV}^2}, \quad (91.5)$$

where E and N are the electromagnetic and color anomalies of the axial current associated with the axion. In grand unified models, and notably for DFSZ [25], $E/N = 8/3$, whereas for KSVZ [24]

$E/N = 0$ if the electric charge of the new heavy quark is taken to vanish. In general, a broad range of E/N values is possible [28, 29], as indicated by the diagonal yellow band in Fig. 91.1. However, this band still does not exhaust all the possibilities. In fact, there exist classes of QCD axion models whose photon couplings populate the entire still allowed region above the yellow band in Fig. 91.1, motivating axion search efforts over a wide range of masses and couplings [30, 31].

The two-photon decay width is

$$\Gamma_{A \rightarrow \gamma\gamma} = \frac{g_{A\gamma\gamma}^2 m_A^3}{64\pi} = 1.1 \times 10^{-24} \text{ s}^{-1} \left(\frac{m_A}{\text{eV}} \right)^5. \quad (91.6)$$

The second expression uses Eq. (91.5) with $E/N = 0$. Axions decay faster than the age of the universe if $m_A \gtrsim 20$ eV. The interaction with fermions f has derivative form and is invariant

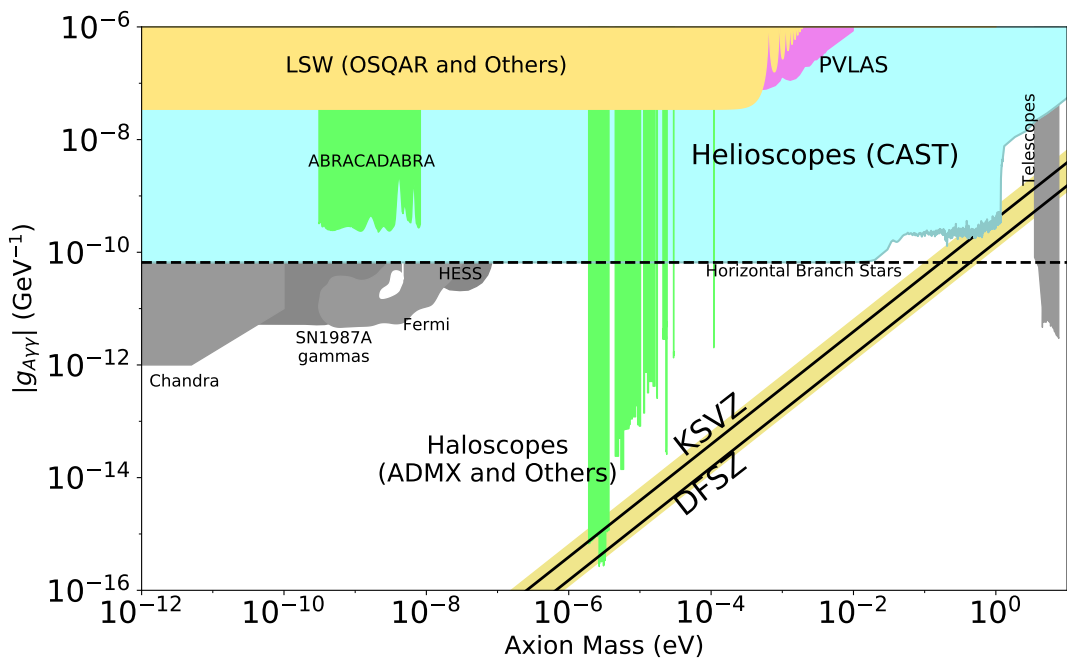


Figure 91.1: Exclusion plot for ALPs as described in the text.

under a shift $\phi_A \rightarrow \phi_A + \phi_0$ as behooves a NG boson,

$$\mathcal{L}_{Aff} = \frac{C_f}{2f_A} \bar{\Psi}_f \gamma^\mu \gamma_5 \Psi_f \partial_\mu \phi_A. \quad (91.7)$$

Here, Ψ_f is the fermion field, m_f its mass, and C_f a model-dependent coefficient. The dimensionless combination $g_{Aff} \equiv C_f m_f / f_A$ plays the role of a Yukawa coupling and $\alpha_{Aff} \equiv g_{Aff}^2 / 4\pi$ of a “fine-structure constant.” The often-used pseudoscalar form $\mathcal{L}_{Aff} = -i(C_f m_f / f_A) \bar{\Psi}_f \gamma_5 \Psi_f \phi_A$ need not be equivalent to the appropriate derivative structure, for example when two NG bosons are attached to one fermion line as in axion emission by nucleon bremsstrahlung [32].

In the DFSZ model [25], the tree-level coupling coefficient to electrons is [33]

$$C_e = \frac{\sin^2 \beta}{3}, \quad (91.8)$$

where $\tan \beta$ is the ratio of the vacuum expectation values of the two Higgs doublets giving masses to the up- and down-type quarks, respectively: $\tan \beta = v_u / v_d$.

For nucleons, $C_{p,n}$ have been determined as [27]

$$\begin{aligned} C_p &= -0.47(3) + 0.88(3)C_u - 0.39(2)C_d - 0.038(5)C_s \\ &\quad - 0.012(5)C_c - 0.009(2)C_b - 0.0035(4)C_t, \\ C_n &= -0.02(3) + 0.88(3)C_d - 0.39(2)C_u - 0.038(5)C_s \\ &\quad - 0.012(5)C_c - 0.009(2)C_b - 0.0035(4)C_t, \end{aligned} \quad (91.9)$$

in terms of the corresponding model-dependent quark couplings C_q , $q = u, d, s, c, b, t$.

For hadronic axions with $C_q = 0$, C_n is compatible with zero whereas C_p does not vanish. In the DFSZ model, on the other hand, $C_u = C_c = C_t = \frac{1}{3} \cos^2 \beta$ and $C_d = C_s = C_b = \frac{1}{3} \sin^2 \beta$, and C_p and C_n , as functions of β ,

$$\begin{aligned} C_p &= -0.435 \sin^2 \beta + (-0.182 \pm 0.025), \\ C_n &= 0.414 \sin^2 \beta + (-0.160 \pm 0.025), \end{aligned} \quad (91.10)$$

do not vanish simultaneously.

The axion-pion interaction is given by the Lagrangian [34]

$$\mathcal{L}_{A\pi} = \frac{C_{A\pi}}{f_\pi f_A} \left(\pi^0 \pi^+ \partial_\mu \pi^- + \pi^0 \pi^- \partial_\mu \pi^+ - 2\pi^+ \pi^- \partial_\mu \pi^0 \right) \partial_\mu \phi_A, \quad (91.11)$$

where $C_{A\pi} = (1 - z)/[3(1 + z)]$ in hadronic models, with $0.38 < z = m_u/m_d < 0.58$ [35, 36]. The chiral symmetry-breaking Lagrangian provides an additional term $\mathcal{L}'_{A\pi} \propto (m_\pi^2/f_\pi f_A) (\pi^0 \pi^0 + 2\pi^- \pi^+) \pi^0 \phi_A$. For hadronic axions it vanishes identically, in contrast to the DFSZ model (Roberto Peccei, private communication).

91.3 Laboratory Searches

91.3.1 Light shining through walls

Searching for “invisible axions” is extremely challenging due to its extraordinarily feeble coupling to normal matter and radiation. Currently, the most promising approaches rely on the axion-two-photon interaction, allowing for axion-photon conversion in external electric or magnetic fields [6]. For the Coulomb field of a charged particle, the conversion is best viewed as a scattering process, $\gamma + Ze \leftrightarrow Ze + A$, called Primakoff effect [37]. In the other extreme of a macroscopic field, usually a large-scale B -field, the momentum transfer is small, the interaction is coherent over a large distance, and the conversion is best viewed as an axion-photon oscillation phenomenon in analogy to neutrino flavor oscillations [38].

Photons propagating through a transverse magnetic field, with incident \mathbf{E}_γ and magnetic field \mathbf{B} parallel, may convert into axions. For $m_A^2 L/2\omega \ll 2\pi$, where L is the length of the B field region and ω the photon energy, the resultant axion beam is coherent with the incident photon beam and the conversion probability is $\Pi \sim (1/4)(g_{A\gamma\gamma} BL)^2$. A practical realization uses a laser beam propagating down the bore of a superconducting dipole magnet (like the bending magnets in high-energy accelerators). If another magnet is in line with the first, but shielded by an optical barrier, then photons may be regenerated from the pure axion beam [39, 40]. The overall probability is $P(\gamma \rightarrow A \rightarrow \gamma) = \Pi^2$.

The first such Light-Shining-through-Walls (LSW) experiment was performed by the BFRT collaboration. It utilized two magnets of length $L = 4.4$ m and $B = 3.7$ T and found $|g_{A\gamma\gamma}| < 6.7 \times 10^{-7} \text{ GeV}^{-1}$ at 95% CL for $m_A < 1$ meV [41]. More recently, several such experiments were performed (see Listings) [42–48]. The current best limit, $|g_{A\gamma\gamma}| < 3.5 \times 10^{-8} \text{ GeV}^{-1}$ at 95% CL for $m_A \lesssim 0.3$ meV (see Fig. 91.1), has been achieved by the OSQAR (Optical Search for QED Vacuum

Birefringence, Axions, and Photon Regeneration) experiment, which exploited two 9 T LHC dipole magnets and an 18.5 W continuous wave laser emitting at the wavelength of 532 nm [48]. Some of these experiments have also reported limits for scalar bosons where the photon \mathbf{E}_γ must be chosen perpendicular to the magnetic field \mathbf{B} .

The concept of resonantly enhanced photon regeneration may open unexplored regions of coupling strength [49, 50]. In this scheme, both the production and detection magnets are within Fabry-Perot optical cavities and actively locked in frequency. The $\gamma \rightarrow A \rightarrow \gamma$ rate is enhanced by a factor $\mathcal{F}\mathcal{F}'/\pi^2$ relative to a single-pass experiment, where \mathcal{F} and \mathcal{F}' are the finesses of the two cavities. The resonant enhancement could be of order $10^{(10-12)}$, improving the $g_{A\gamma\gamma}$ sensitivity by $10^{(2.5-3)}$. The experiment ALPS II (Any Light Particle Search II) is based on this concept and aims at an improvement of the current laboratory bound on $g_{A\gamma\gamma}$ by a factor $\sim 10^3$ in the year 2020 [51].

Resonantly enhanced photon regeneration has already been exploited in experiments searching for ‘radiowaves shining through a shielding’ [52–55]. For $m_A \lesssim 10^{-5}$ eV, the upper bound on $g_{A\gamma\gamma}$ established by the CROWS (CERN Resonant Weakly Interacting sub-eV Particle Search) experiment [56] is slightly less stringent than the one set by OSQAR.

91.3.2 Photon polarization

An alternative to regenerating the lost photons is to use the beam itself to detect conversion: the polarization of light propagating through a transverse B field suffers dichroism and birefringence [57]. Dichroism: The E_{\parallel} component, but not E_{\perp} , is depleted by axion production, causing a small rotation of linearly polarized light. For $m_A^2 L/2\omega \ll 2\pi$, the effect is independent of m_A . For heavier axions, it oscillates and diminishes as m_A increases, and it vanishes for $m_A > \omega$. Birefringence: This effect occurs because there is mixing of virtual axions in the E_{\parallel} state, but not for E_{\perp} . Hence, linearly polarized light will develop elliptical polarization. Higher-order QED also induces vacuum magnetic birefringence (VMB). A search for these effects was performed in the same dipole magnets of the BFRT experiment mentioned before [58]. The dichroic rotation gave a stronger limit than the ellipticity rotation: $|g_{A\gamma\gamma}| < 3.6 \times 10^{-7} \text{ GeV}^{-1}$ at 95% CL, for $m_A < 5 \times 10^{-4}$ eV. The ellipticity limits are better at higher masses, as they fall off smoothly and do not terminate at m_A .

In 2006, the PVLAS collaboration reported a signature of magnetically induced vacuum dichroism that could be interpreted as the effect of a pseudoscalar with $m_A = 1\text{--}1.5$ meV and $|g_{A\gamma\gamma}| = (1.6\text{--}5) \times 10^{-6} \text{ GeV}^{-1}$ [59]. Later, it turned out that these findings are due to instrumental artifacts [60]. This particle interpretation is also excluded by the above photon regeneration searches that were inspired by the original PVLAS result. The fourth generation setup of the PVLAS experiment has published results on searches for VMB (see Fig. 91.1) and dichroism [61]. The bounds from the non-observation of the latter on $g_{A\gamma\gamma}$ are slightly weaker than the ones from OSQAR.

91.3.3 Long-range forces

New bosons would mediate long-range forces, which are severely constrained by ‘fifth force’ experiments [62]. Those looking for new mass-spin couplings provide significant constraints on pseudoscalar bosons [63]. Presently, the most restrictive limits are obtained from combining long-range force measurements with stellar cooling arguments [64]. For the moment, any of these limits are far from realistic values expected for axions. Still, these efforts provide constraints on more general low-mass bosons.

In Ref. [65], a method was proposed that can extend the search for axion-mediated spin-dependent forces by several orders of magnitude. By combining techniques used in nuclear magnetic resonance and short-distance tests of gravity, this method appears to be sensitive to axions in the $\mu\text{eV} - \text{meV}$ mass range, independent of the cosmic axion abundance, if axions have a CP-violating interaction with nuclei as large as the current experimental bound on the electric dipole moment

of the neutron allows. Experimental tests to demonstrate the requirements of ARIADNE (Axion Resonant InterAction DetectioN Experiment) are under way [66].

91.4 Axions from Astrophysical Sources

91.4.1 Stellar energy-loss limits

Low-mass weakly-interacting particles (neutrinos, gravitons, axions, baryonic or leptonic gauge bosons, *etc.*) are produced in hot astrophysical plasmas, and can thus transport energy out of stars. The coupling strength of these particles with normal matter and radiation is bounded by the constraint that stellar lifetimes or energy-loss rates are not in conflict with observation [67, 68].

We begin this discussion with our Sun and concentrate on hadronic axions. They are produced predominantly by the Primakoff process $\gamma + Ze \rightarrow Ze + A$. Integrating over a standard solar model yields the axion luminosity [69]

$$L_A = g_{10}^2 \times 1.85 \times 10^{-3} L_\odot, \quad (91.12)$$

where $g_{10} = |g_{A\gamma\gamma}| \times 10^{10}$ GeV. The maximum of the spectrum is at 3.0 keV, the average at 4.2 keV, and the number flux at Earth is $g_{10}^2 \times 3.75 \times 10^{11}$ cm⁻² s⁻¹. The solar photon luminosity is fixed, so energy losses due to the Primakoff process require enhanced nuclear energy production and thus enhanced neutrino fluxes. The all-flavor measurements by SNO (Solar Neutrino Observatory), together with a standard solar model, imply $L_A \lesssim 0.10 L_\odot$, corresponding to $g_{10} \lesssim 7$ [70], mildly superseding a similar limit from helioseismology [71]. In Ref. [72], this limit was improved to $g_{10} < 4.1$ (at 3σ), exploiting a new statistical analysis that combined helioseismology (sound speed, surface helium and convective radius) and solar neutrino observations, including theoretical and observational errors, and accounting for tensions between input parameters of solar models, in particular the solar element abundances.

A more restrictive limit derives from globular-cluster (GC) stars that allow for detailed tests of stellar-evolution theory. The stars on the horizontal branch (HB) in the color-magnitude diagram have reached helium burning with a core-averaged energy release of about 80 erg g⁻¹ s⁻¹, compared to Primakoff axion losses of $g_{10}^2 30$ erg g⁻¹ s⁻¹. The accelerated consumption of helium reduces the HB lifetime by about $80/(80 + 30 g_{10}^2)$. Number counts of HB stars in a large sample of 39 Galactic GCs compared with the number of red giants (that are not much affected by Primakoff losses) give a weak indication of non-standard losses which may be accounted by Primakoff-like axion emission, if the photon coupling is in the range $|g_{A\gamma\gamma}| = (2.9 \pm 1.8) \times 10^{-11}$ GeV⁻¹ [73, 74]. Still, the upper bound found in this analysis,

$$|g_{A\gamma\gamma}| < 6.6 \times 10^{-11} \text{ GeV}^{-1} \text{ (95\% CL)}, \quad (91.13)$$

represents the strongest limit on $g_{A\gamma\gamma}$ for a wide mass range, see Fig. 91.1. The conservative constraint, Eq. (91.13), on $g_{A\gamma\gamma}$ may be translated to $f_A > 3.4 \times 10^7$ GeV ($m_A < 0.2$ eV), using $E/N = 0$ as in the KSVZ model, or to $f_A > 1.3 \times 10^7$ GeV ($m_A < 0.5$ eV), for the DFSZ axion model, with $E/N = 8/3$, see Fig. 91.1.

If axions couple directly to electrons, the dominant emission processes are atomic axio-recombination and axio-deexcitation, axio-bremsstrahlung in electron-ion or electron-electron collisions, and Compton scattering [75]. Stars in the red giant (RG) branch of the color-magnitude diagram of GCs are particularly sensitive to these processes. In fact, they would lead to an extension of the latter to larger brightness. Reference [76] provided high-precision photometry for the Galactic globular cluster M5 (NGC 5904), allowing for a detailed comparison between the observed tip of the RG branch with predictions based on state-of-the-art stellar evolution theory. It was found that, within the uncertainties, the observed and predicted tip of the RG branch brightness agree

reasonably well, leading to the bound

$$|g_{Aee}| < 4.3 \times 10^{-13} \quad (95\% \text{ CL}), \quad (91.14)$$

implying an upper bound on the axion mass in the DFSZ model,

$$m_A \sin^2 \beta < 15 \text{ meV} \quad (95\% \text{ CL}), \quad (91.15)$$

see Fig. 91.2 (left panel). Intriguingly, the agreement would improve with a small amount of extra cooling that slightly postpones helium ignition, preferring an electron coupling around $|g_{Aee}| \sim 1.9 \times 10^{-13}$, corresponding to $m_A \sin^2 \beta \sim 7 \text{ meV}$.

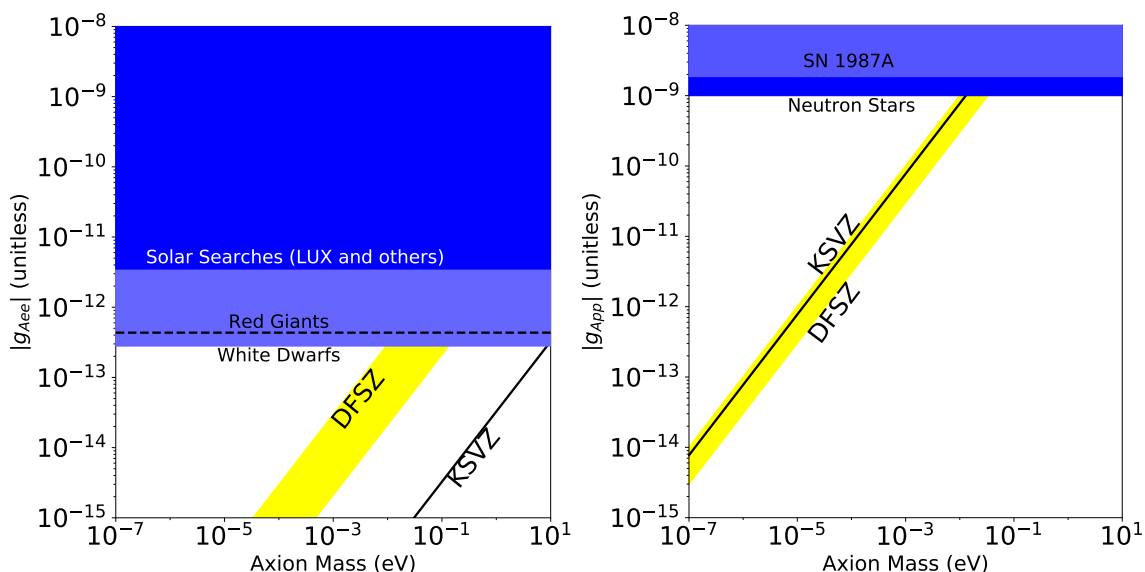


Figure 91.2: Exclusion plots for ALPs as described in the text. For the DFSZ range we have taken into account the constraint $0.28 \lesssim \tan \beta \lesssim 140$ [77] arising from the requirement of perturbative unitarity of the Yukawa couplings of Standard Model fermions.

Bremsstrahlung is also efficient in white dwarfs (WDs), where the Primakoff and Compton processes are suppressed by the large plasma frequency. A comparison of the predicted and observed luminosity function of WDs can be used to put limits on $|g_{Aee}|$ [78]. A recent analysis, based on detailed WD cooling treatment and new data on the WD luminosity function (WDLF) of the Galactic Disk, found that electron couplings above $|g_{Aee}| \gtrsim 3 \times 10^{-13}$, corresponding to a DFSZ axion mass $m_A \sin^2 \beta \gtrsim 10 \text{ meV}$, are disfavoured [79], see Fig. 91.2 (left panel). Lower couplings cannot be discarded from the current knowledge of the WDLF of the Galactic Disk. On the contrary, features in some WDLFs can be interpreted as suggestions for electron couplings in the range $7.2 \times 10^{-14} \lesssim |g_{Aee}| \lesssim 2.2 \times 10^{-13}$, corresponding to $2.5 \text{ meV} \lesssim m_A \sin^2 \beta \lesssim 7.5 \text{ meV}$ [79, 80]. This hypothesis will be further scrutinized by the Large Synoptic Survey Telescope (LSST) which is expected to increase the sample of WDs in the Galactic halo to hundreds of thousands [81]. This will allow for the determination of independent WDLFs from different Galactic populations, greatly reducing the uncertainties related to star formation histories. For pulsationally unstable WDs (ZZ Ceti stars), the period decrease \dot{P}/P is a measure of the cooling speed. The corresponding observations of the pulsating WDs G117-B15A and R548 imply additional cooling that can be interpreted also in terms of similar axion losses [82, 83].

Recently, it has been pointed out that the hints of excessive cooling of WDs, RGs and HB stars can be explained at one stroke by an ALP coupling to electrons and photons, with couplings $|g_{Aee}| \sim 1.5 \times 10^{-13}$ and $|g_{A\gamma\gamma}| \sim 1.4 \times 10^{-11} \text{ GeV}^{-1}$, respectively [84, 85]. Intriguingly, good fits to the data can be obtained employing the DFSZ axion with a mass in the range $4 \text{ meV} \lesssim m_A \lesssim 250 \text{ meV}$ [84].

Similar constraints derive from the measured duration of the neutrino signal of the supernova SN 1987A. Numerical simulations for a variety of cases, including axions and Kaluza-Klein gravitons, reveal that the energy-loss rate of a nuclear medium at the density $3 \times 10^{14} \text{ g cm}^{-3}$ and temperature 30 MeV should not exceed about $1 \times 10^{19} \text{ erg g}^{-1} \text{ s}^{-1}$ [86]. The energy-loss rate from nucleon bremsstrahlung, $N + N \rightarrow N + N + A$, is $(C_N/2f_A)^2(T^4/\pi^2 m_N) F$. Here F is a numerical factor that represents an integral over the dynamical spin-density structure function because axions couple to the nucleon spin. For realistic conditions, even after considerable effort, one is limited to a heuristic estimate leading to $F \approx 1$ [68]. The SN 1987A limits are of particular interest for hadronic axions where the bounds on $|g_{Aee}|$ are moot. Using a proton fraction of 0.3, $g_{Ann} = 0$, $F = 1$, and $T = 30 \text{ MeV}$, one finds $f_A \gtrsim 4 \times 10^8 \text{ GeV}$ and $m_A \lesssim 16 \text{ meV}$ [68], see Fig. 91.2 (right panel). A more detailed numerical calculation [87] with state of the art SN models, again assuming $g_{Ann} = 0$, found that a coupling larger than $|g_{App}| \gtrsim 6 \times 10^{-10}$, would shorten significantly the timescale of the neutrino emission. This result is, not surprisingly, rather close to the estimate in Ref. [68]. Improving the calculation of axion emission via nucleon-nucleon bremsstrahlung beyond the basic one-pion exchange approximation appears to loosen the bound [88, 89]. The latter analysis finds a reduction of the axion emissivity by an order of magnitude if one takes into account the non-vanishing mass of the exchanged pion, the contribution from two-pion exchange, effective in-medium nucleon masses and multiple nucleon scattering, leading to a looser bound (Maurizio Giannotti and Alessandro Mirizzi, private communication)

$$g_{Ann}^2 + 0.29 g_{App}^2 + 0.27 g_{Ann} g_{App} < 3.25 \times 10^{-18}. \quad (91.16)$$

However, with the present understanding of SNe (current lack of self-consistent 3D SN simulations) and the sparse data from SN 1987A, the constraint on the axion-nucleon couplings from SN 1987A should be considered more as indicative than as a sharp bound [87].

If axions interact sufficiently strongly they are trapped. Only about three orders of magnitude in g_{ANN} or m_A are excluded. For even larger couplings, the axion flux would have been negligible, yet it would have triggered additional events in the detectors, excluding a further range [90]. A possible gap between these two SN 1987A arguments was discussed as the ‘‘hadronic axion window’’ under the assumption that $g_{A\gamma\gamma}$ was anomalously small [91]. This range is now excluded by hot dark matter (HDM) bounds (see below).

There is another hint for excessive stellar energy losses from the neutron star (NS) in the supernova remnant Cassiopeia A (Cas A): its surface temperature measured over 10 years reveals an unusually fast cooling rate. This rapid cooling of the Cas A NS may be explained by NS minimal cooling with neutron superfluidity and proton superconductivity [92, 93]. The rapid cooling may also arise from a phase transition of the neutron condensate into a multicomponent state [94]. Recently, Ref. [95] analyzed Cas A NS cooling in the presence of axion emission and obtained

$$g_{App}^2 + 1.6 g_{Ann}^2 < 1 \times 10^{-18}, \quad (91.17)$$

which is comparable to the SN 1987A bound. Refs. [96] put a more conservative bound without an attempt to fit a transient behavior of Cas A,

$$g_{App}^2 < (1 - 6) \times 10^{-17} \text{ (or } f_A > (5 - 10) \times 10^7 \text{ GeV)}, \quad (91.18)$$

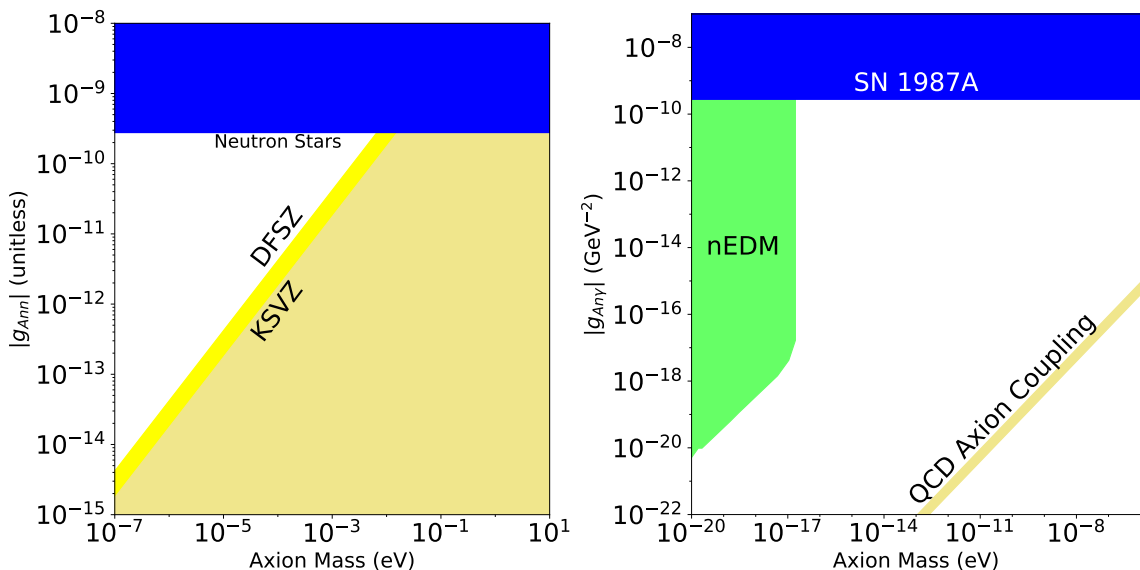


Figure 91.3: Exclusion plots for ALPs as described in the text.

from the temperatures of Cas A and other NSs. The Cas A NS cooling may also be interpreted as a hint for extra cooling caused by the emission of axions from the breaking and re-formation of neutron triplet Cooper pairs [97], requiring a coupling to the neutron of

$$g_{Ann}^2 = (1.4 \pm 0.5) \times 10^{-19}, \quad (91.19)$$

corresponding to an axion mass

$$m_A = (2.3 \pm 0.4) \text{ meV}/C_n. \quad (91.20)$$

On the other hand, Ref. [98] considered another hot young NS in the supernova remnant HESS J1731-347. Its high temperature implies that all the neutrino emission processes except neutron-neutron bremsstrahlung must be strongly suppressed, which can be realized with a negligible neutron triplet gap and a large proton singlet gap. In this setup, the bremsstrahlung from neutrons is the dominant channel for axion emission, from which one obtains a limit

$$g_{Ann}^2 < 7.7 \times 10^{-20}, \quad (91.21)$$

see Fig. 91.3 (left panel).

Finally, let us note that if the interpretation of the various hints for additional cooling of stars reported in this section in terms of emission of axions with $m_A \sim \text{meV}$ were correct, SNe would lose a large fraction of their energy as axions. This would lead to a diffuse SN axion background in the universe with an energy density comparable to the extra-galactic background light [99]. However, there is no apparent way of detecting it or the axion burst from the next nearby SN. On the other hand, neutrino detectors such as IceCube, Super-Kamiokande or a future mega-ton water Cherenkov detector will probe exactly the mass region of interest by measuring the neutrino pulse duration of the next galactic SN [87].

91.4.2 Searches for solar axions and ALPs

Instead of using stellar energy losses to derive axion limits, one can also search directly for these fluxes, notably from the Sun. The main focus has been on ALPs with a two-photon vertex. They

are produced by the Primakoff process with a flux given by Eq. (91.12) and an average energy of 4.2 keV, and can be detected at Earth with the reverse process in a macroscopic B -field (“axion helioscope”) [6]. In order to extend the sensitivity in mass towards larger values, one can endow the photon with an effective mass in a gas, $m_\gamma = \omega_{\text{plas}}$, thus matching the axion and photon dispersion relations [100].

An early implementation of these ideas used a conventional dipole magnet, with a conversion volume of variable-pressure gas with a xenon proportional chamber as x-ray detector [101]. The conversion magnet was fixed in orientation and collected data for about 1000 s/day. Axions were excluded for $|g_{A\gamma\gamma}| < 3.6 \times 10^{-9} \text{ GeV}^{-1}$ for $m_A < 0.03 \text{ eV}$, and $|g_{A\gamma\gamma}| < 7.7 \times 10^{-9} \text{ GeV}^{-1}$ for $0.03 < m_A < 0.11 \text{ eV}$ at 95% CL.

Later, the Tokyo axion helioscope used a superconducting magnet on a tracking mount, viewing the Sun continuously. They reported $|g_{A\gamma\gamma}| < 6 \times 10^{-10} \text{ GeV}^{-1}$ for $m_A < 0.3 \text{ eV}$ [102]. This experiment was recommissioned and a similar limit for masses around 1 eV was reported [103].

The most recent helioscope CAST (CERN Axion Solar Telescope) uses a decommissioned LHC dipole magnet on a tracking mount. The hardware includes grazing-incidence x-ray optics with solid-state x-ray detectors, as well as novel x-ray Micromegas position-sensitive gaseous detectors. Exploiting a IAXO (see below) pathfinder system, CAST has established the limit

$$|g_{A\gamma\gamma}| < 6.6 \times 10^{-11} \text{ GeV}^{-1} \quad (95\% \text{ CL}), \quad (91.22)$$

for $m_A < 0.02 \text{ eV}$ [104]. To cover larger masses, the magnet bores are filled with a gas at varying pressure. The runs with ^4He cover masses up to about 0.4 eV [105], providing the ^4He limits shown in Fig. 91.1. To cover yet larger masses, ^3He was used to achieve a larger pressure at cryogenic temperatures. Limits up to 1.17 eV allowed CAST to “cross the axion line” for the KSVZ model [106], see Fig. 91.1.

Going to yet larger masses in a helioscope search is not well motivated because of the cosmic HDM bound of $m_A \lesssim 1 \text{ eV}$ (see below). Sensitivity to significantly smaller values of $g_{A\gamma\gamma}$ can be achieved with a next-generation axion helioscope with a much larger magnetic-field cross section. Realistic design options for this “International Axion Observatory” (IAXO) have been studied in some detail [107] and its physics potential has been reviewed recently [108]. Such a next-generation axion helioscope may also push the sensitivity in the product of couplings to photons and to electrons, $g_{A\gamma\gamma}g_{Aee}$, into a range beyond stellar energy-loss limits and test the hypothesis that WD, RG, and HB cooling is dominated by axion emission [84, 109]. As a first step towards IAXO, an intermediate experimental stage called BabyIAXO is currently under preparation at DESY (for a short introduction, see Ref. [108]).

Other Primakoff searches for solar axions and ALPs have been carried out using crystal detectors, exploiting the coherent conversion of axions into photons when the axion angle of incidence satisfies a Bragg condition with a crystal plane [110]. However, none of these limits is more restrictive than the one derived from the constraint on the solar axion luminosity ($L_A \lesssim 0.10 L_\odot$) discussed earlier.

Another idea is to look at the Sun with an x-ray satellite when the Earth is in between. Solar axions and ALPs would convert in the Earth magnetic field on the far side and could be detected [111]. The sensitivity to $g_{A\gamma\gamma}$ could be comparable to CAST, but only for much smaller m_A . Deep solar x-ray measurements with existing satellites, using the solar magnetosphere as conversion region, have reported preliminary limits on $g_{A\gamma\gamma}$ [112].

Direct detection experiments searching for dark matter (DM) consisting of weakly interacting massive particles, such as EDELWEISS-II, LUX, and XENON100, have also the capability to search for solar axions and ALPs [113, 114]. Recently, the LUX experiment [114] has put a bound on the

axion-electron coupling constant by exploiting the axio-electric effect in liquid xenon,

$$|g_{Aee}| < 3.5 \times 10^{-12} \quad (90\% \text{ CL}), \quad (91.23)$$

excluding the DFSZ model with $m_A \sin^2 \beta > 0.12 \text{ eV}$, cf. see Fig. 91.2 (left panel). However, as obvious from the same figure, this technique has not reached the sensitivity of energy-loss considerations in stars (RGs and WDs).

91.4.3 Conversion of astrophysical photon fluxes

Large-scale B fields exist in astrophysics that can induce axion-photon oscillations. In practical cases, B is much smaller than in the laboratory, whereas the conversion region L is much larger. Therefore, while the product BL can be large, realistic sensitivities are usually restricted to very low-mass particles, far away from the ‘‘axion band’’ in a plot like Fig. 91.1.

One example is SN 1987A, which would have emitted a burst of ALPs due to the Primakoff production in its core. They would have partially converted into γ -rays in the galactic B -field. The lack of a gamma-ray signal in the GRS instrument of the SMM satellite in coincidence with the observation of the neutrinos emitted from SN 1987A therefore provides a strong bound on their coupling to photons [115]. This bound has been revisited and the underlying physics has been brought to the current state-of-the-art, as far as modelling of the supernova and the Milky-Way magnetic field are concerned, resulting in the limit [116]

$$|g_{A\gamma\gamma}| < 5.3 \times 10^{-12} \text{ GeV}^{-1}, \text{ for } m_A \lesssim 4.4 \times 10^{-10} \text{ eV}, \quad (91.24)$$

see Fig. 91.1. Magnetically induced oscillations between photons and ALPs can modify the photon fluxes from distant sources in various ways, featuring (i) frequency-dependent dimming, (ii) modified polarization, and (iii) avoiding absorption by propagation in the form of axions.

For example, dimming of SNe Ia could influence the interpretation in terms of cosmic acceleration [117], although it has become clear that photon-ALP conversion could only be a subdominant effect [118]. Searches for linearly polarised emission from magnetised white dwarfs [119] and changes of the linear polarisation from radio galaxies (see, e.g., Ref. [120]) provide limits close to $g_{A\gamma\gamma} \sim 10^{-11} \text{ GeV}^{-1}$, for masses $m_A \lesssim 10^{-7} \text{ eV}$ and $m_A \lesssim 10^{-15} \text{ eV}$, respectively, albeit with uncertainties related to the underlying assumptions. Even stronger limits, $g_{A\gamma\gamma} \lesssim 2 \times 10^{-13} \text{ GeV}^{-1}$, for $m_A \lesssim 10^{-14} \text{ eV}$, have been obtained by exploiting high-precision measurements of quasar polarisations [121].

Remarkably, it appears that the universe could be too transparent to TeV γ -rays that should be absorbed by pair production on the extra-galactic background light [122–126]. The situation is not conclusive at present [127–129], but the possible role of photon-ALP oscillations in TeV γ -ray astronomy is tantalizing [130]. Fortunately, the region in ALP parameter space, $g_{A\gamma\gamma} \sim 10^{-12} - 10^{-10} \text{ GeV}^{-1}$ for $m_A \lesssim 10^{-7} \text{ eV}$ [131], required to explain the anomalous TeV transparency of the universe, could be conceivably probed by the next generation of laboratory experiments (ALPS II) and helioscopes (IAXO) mentioned above. This parameter region can also be probed by searching for an irregular behavior of the gamma ray spectrum of distant active galactic nuclei (AGN), expected to arise from photon-ALP mixing in a limited energy range. The H.E.S.S. collaboration has set a limit of $|g_{A\gamma\gamma}| \lesssim 2.1 \times 10^{-11} \text{ GeV}^{-1}$, for $1.5 \times 10^{-8} \text{ eV} \lesssim m_A \lesssim 6.0 \times 10^{-8} \text{ eV}$, from the non-observation of an irregular behavior of the spectrum of the AGN PKS 2155-304 [132], see Fig. 91.1. The Fermi-LAT collaboration has put an even more stringent limit on the ALP-photon coupling [133] from observations of the gamma ray spectrum of NGC 1275, the central galaxy of the Perseus cluster, see Fig. 91.1. A similar analysis has been carried out in Ref. [134] using Fermi-LAT data of PKS 2155-304.

Evidence for spectral irregularities has been reported in Galactic sources, such as pulsars and supernova remnants, and has been interpreted as hints for ALPs [135, 136]. However, the inferred ALP parameters are in tension with the CAST helioscope bounds. It should also be noted that the high signal-to-noise spectra of Galactic gamma-ray sources are dominated by uncertainties of the instrumental systematics rather than statistical errors. Furthermore, it has been shown that additional care has to be taken when deriving confidence intervals on ALP parameters based on Wilks' theorem [137], since it has been shown that it does not apply for testing the ALP hypothesis [133].

At smaller masses, $m_A \lesssim 10^{-12}$ eV, galaxy clusters become highly efficient at interconverting ALPs and photons at x-ray energies. Constraints on spectral irregularities in the spectra of luminous x-ray sources (Hydra A, M87, NGC 1275, NGC 3862, Seyfert galaxy 2E3140; taken by Chandra and XMM-Newton) located in or behind galaxy clusters then lead to stringent upper limits on the ALP-photon coupling [138–143]. In this type of studies, the uncertainty in the cluster magnetic field needs to be taken into account. This typically leads to a range of limits on the ALP-photon coupling that depend on the modelling assumptions. Reference [143] recently performed the most sensitive x-ray searches for ALPs to date by employing Chandra's High-Energy Transmission Gratings that allow for an unsurpassed spectral resolution. New observations of the AGN NGC 1275 then led to the bound

$$|g_{A\gamma\gamma}| < 8 \times 10^{-13} \text{ GeV}^{-1} \quad (99.7\% \text{ CL}) \quad (91.25)$$

for light ALPs, see Fig. 91.1.

91.4.4 Superradiance of black holes

Light bosonic fields such as axions or ALPs can affect the dynamics and gravitational wave emission of rapidly rotating astrophysical black holes through the superradiance mechanism. When their Compton wavelength is of order of the black hole size, they form gravitational bound states around the black hole. Their occupation number grows exponentially by extracting energy and angular momentum from the black hole, forming a coherent axion or ALP bound state emitting gravitational waves. When accretion cannot replenish the spin of the black hole, superradiance dominates the black hole spin evolution; this is true for both supermassive and stellar mass black holes. The existence of destabilizing light bosonic fields thus leads to gaps in the mass vs. spin plot of rotating black holes. Stellar black hole spin measurements – exploiting well-studied binaries and two independent techniques – exclude a mass range $6 \times 10^{-13} \text{ eV} < m_A < 2 \times 10^{-11} \text{ eV}$ at 2σ , which for the axion excludes $3 \times 10^{17} \text{ GeV} < f_A < 1 \times 10^{19} \text{ GeV}$ [11, 144, 145]. These bounds apply when gravitational interactions dominate over the axion self-interaction, which is true for the QCD axion in this mass range. Long lasting, monochromatic gravitational wave signals, which can be distinguished from ordinary astrophysical sources by their clustering in a narrow frequency range, are expected to be produced by axions or ALPs annihilating to gravitons. Gravitational waves could also be sourced by axions/ALPs transitioning between gravitationally bound levels. Accordingly, the gravitational wave detector Advanced LIGO should be sensitive to the axion in the $m_A \lesssim 10^{-10}$ eV region. LIGO measurements of black hole spins in binary merger events could also provide statistical evidence for the presence of an axion [146, 147]. Similar signatures could arise for supermassive black holes for particle with masses $\lesssim 10^{-15}$ eV. Gravitational waves from such sources could be detected at lower-frequency observatories such as LISA.

91.5 Cosmic Axions

91.5.1 Cosmic axion populations

In the early universe, axions are produced by processes involving quarks and gluons [148]. After color confinement, the dominant thermalization process is $\pi + \pi \leftrightarrow \pi + A$ [34]. The resulting axion

population would contribute an HDM component in analogy to massive neutrinos. Cosmological precision data provide restrictive constraints on a possible HDM fraction that translate into $m_A \lesssim 1$ eV [149], but in detail depend on the used data set and assumed cosmological model. In the future, data from a EUCLID-like survey combined with Planck CMB data can detect HDM axions with a mass $m_A \gtrsim 0.15$ eV at very high significance [150].

For $m_A \gtrsim 20$ eV, axions decay fast on a cosmic time scale, removing the axion population while injecting photons. This excess radiation provides additional limits up to very large axion masses [151]. An anomalously small $g_{A\gamma\gamma}$ provides no loophole because suppressing decays leads to thermal axions overdominating the mass density of the universe.

The main cosmological interest in axions derives from their possible role as CDM. In addition to thermal processes, axions are abundantly produced by the vacuum re-alignment (VR) mechanism [152].

The axion DM abundance crucially depends on the cosmological history. Let us first consider the so called *pre-inflationary PQ symmetry breaking scenario*, in which the PQ symmetry is broken before and during inflation and not restored afterwards. After the breakdown of the PQ symmetry, the axion field relaxes somewhere in the bottom of the “wine-bottle-bottom” potential. Near the QCD epoch, topological fluctuations of the gluon fields such as instantons explicitly break the PQ symmetry. This tilting of the “wine-bottle-bottom” drives the axion field toward the CP-conserving minimum, thereby exciting coherent oscillations of the axion field that ultimately represent a condensate of CDM. The fractional cosmic mass density in this homogeneous field mode, created by the VR mechanism, is [23, 153–155],

$$\begin{aligned} \Omega_A^{\text{VR}} h^2 &\approx 0.12 \left(\frac{f_A}{9 \times 10^{11} \text{ GeV}} \right)^{1.165} F \Theta_i^2 \\ &\approx 0.12 \left(\frac{6 \mu\text{eV}}{m_A} \right)^{1.165} F \Theta_i^2, \end{aligned} \quad (91.26)$$

where h is the present-day Hubble expansion parameter in units of $100 \text{ km s}^{-1} \text{ Mpc}^{-1}$, and $-\pi \leq \Theta_i \leq \pi$ is the initial “misalignment angle” relative to the CP-conserving position attained in the causally connected region which evolved into today’s observable universe. $F = F(\Theta_i, f_A)$ is a factor accounting for anharmonicities in the axion potential. For $F\Theta_i^2 = \mathcal{O}(1)$, m_A should be above $\sim 6 \mu\text{eV}$ in order that the cosmic axion density does not exceed the observed CDM density, $\Omega_{\text{CDM}} h^2 = 0.12$. However, much smaller axion masses (much higher PQ scales) are still possible if the initial value Θ_i just happens to be small enough in today’s observable universe (“anthropic axion window” [156]). In this cosmological scenario, however, quantum fluctuations of the axion field during inflation are expected to lead to isocurvature density fluctuations which get imprinted to the temperature fluctuations of the CMB [157, 158]. Their non-observation puts severe constraints on the Hubble expansion rate H_I during inflation [159–163], which read, in the simplest cosmological inflationary scenario,

$$H_I \lesssim 5.7 \times 10^8 \text{ GeV} \left(\frac{5 \text{ neV}}{m_a} \right)^{0.4175}, \quad (91.27)$$

if axions represent all of DM.

In the *post-inflationary PQ symmetry breaking scenario*, on the other hand, Θ_i will take on different values in different patches of the present universe. The average contribution is [23, 153–155]

$$\Omega_A^{\text{VR}} h^2 \approx 0.12 \left(\frac{30 \mu\text{eV}}{m_A} \right)^{1.165}. \quad (91.28)$$

The decay of cosmic strings and domain walls gives rise to a further population of CDM axions, whose abundance suffers from significant uncertainties [154, 155, 164–172] which arise from the

difficulty in understanding the energy loss process of topological defects and the generated axion spectrum in a quantitative way. In fact, in the present state-of-the-art it is still possible that the CDM contribution from the decay of topological defects is subdominant or overwhelmingly large in comparison to the one from the VR mechanism. Correspondingly, the plausible range of axion masses providing all of CDM in scenarios with postinflationary PQ symmetry breaking is still rather large, namely

$$m_A \approx 25 \mu\text{eV} - 4.4 \text{ meV}, \quad (91.29)$$

for models with short-lived (requiring unit color anomaly $N = 1$) domain walls, such as the KSVZ model. For models with long-lived ($N > 1$) domain walls, such as an accidental DFSZ model [173], where the PQ symmetry is broken by higher dimensional Planck suppressed operators, the mass is predicted to be significantly higher [168, 173, 174],

$$m_A \approx (0.58 - 130) \text{ meV}. \quad (91.30)$$

However, the upper part of the predicted range is in conflict with stellar energy-loss limits on the axion, cf. Fig. 91.2 (right panel) and Fig. 91.3 (left panel).

In this post-inflationary PQ symmetry breakdown scenario, the spatial axion density variations are large at the QCD transition and they are not erased by free streaming. Gravitationally bound “axion miniclusters” form before and around matter-radiation equality [175–177]. A significant fraction of CDM axions can reside in these bound objects [171, 178]. Remarkably, the minicluster fraction can be bounded by gravitational lensing [179–181].

In the above predictions of the fractional cosmic mass density in axions, the exponent, 1.165, arises from the non-trivial temperature dependence of the topological susceptibility $\chi(T) = m_A^2(T) f_A^2$ at temperatures slightly above the QCD quark-hadron phase transition. Lattice QCD calculations of this exponent [23, 182–186], but also Ref. [187], found it to be remarkably close to the prediction of the dilute instanton gas approximation [188] which was previously exploited. Therefore, the state-of-the-art prediction of the axion mass relevant for DM for a fixed initial misalignment angle Θ_i differs from the previous prediction by just a factor of order one.

The non-thermal production mechanisms attributed to axions are generic to light bosonic weakly interacting particles such as ALPs [189]. The relic abundance is set by the epoch when the axion mass becomes significant, $3H(t) \approx m_A(t)$, and ALP field oscillations begin. For ALPs to contribute to the DM density this epoch must precede that of matter radiation equality. For a temperature independent ALP mass this leads to the bound:

$$m_A \gtrsim 7 \times 10^{-28} \text{ eV} \left(\frac{\Omega_m h^2}{0.15} \right)^{1/2} \left(\frac{1 + z_{\text{eq}}}{3.4 \times 10^3} \right)^{3/2}. \quad (91.31)$$

ALPs lighter than this bound are allowed if their cosmic energy density is small, but they are quite distinct from other forms of DM [190]. Ignoring anharmonicities in the ALP potential, and taking the ALP mass to be temperature independent, the relic density in DM ALPs due to the VR mechanism is given by

$$\Omega_{\text{ALP}}^{\text{VR}} h^2 = 0.12 \left(\frac{m_A}{4.7 \times 10^{-19} \text{ eV}} \right)^{1/2} \left(\frac{f_A}{10^{16} \text{ GeV}} \right)^2 \left(\frac{\Omega_m h^2}{0.15} \right)^{3/4} \left(\frac{1 + z_{\text{eq}}}{3.4 \times 10^3} \right)^{-3/4} \Theta_i^2. \quad (91.32)$$

An ALP decay constant near the GUT scale gives the correct relic abundance for *ultralight ALPs* (ULAs), which we now define. Extended discussions of ULAs can be found in Refs. [191, 192].

The standard CDM model treats DM as a distribution of cold, collisionless particles interacting only via gravity. Below the Compton wavelength, $\lambda_c = 2\pi/m_A$, the particle description of ALPs

breaks down. For large occupation numbers we can model ALPs below the Compton wavelength as a coherent classical field. Taking as a reference length scale the Earth radius, $R_{\oplus} = 6371$ km, we define ULAs to be those axions with $\lambda_c > R_{\oplus}$, leading to the defining bound

$$m_{\text{ULA}} < 2 \times 10^{-13} \text{ eV}. \quad (91.33)$$

ULAs encompass the entire Earth in a single coherent field. The coherence time of the ULA field on Earth can be estimated from the crossing time of the de Broglie wavelength at the virial velocity in the Milky Way, $\tau_{\text{coh.}} \sim 1/m_{\text{ULA}} v_{\text{vir.}}^2$.

We notice that by the definition, Eq. (91.33), an ultralight QCD axion must have a super-Planckian decay constant, $f_A > 3 \times 10^{19}$ GeV and would require fine tuning of θ_i to provide the relic abundance. Natural models for ULAs can be found in string and M-theory compactifications [7–14], in field theory with accidental symmetries [193], or new hidden strongly coupled sectors [194].

In addition to the gravitational potential energy, the ULA field also carries gradient energy. On scales where the gradient energy is non-negligible, ULAs acquire an effective pressure and do not behave as CDM. The gradient energy opposes gravitational collapse, leading to a Jeans scale below which perturbations are stable [195]. The Jeans scale suppresses linear cosmological structure formation relative to CDM [196]. The Jeans scale at matter-radiation equality in the case that ULAs make up all of CDM is:

$$k_{\text{J,eq}} = 8.7 \text{ Mpc}^{-1} \left(\frac{1 + z_{\text{eq}}}{3.4 \times 10^3} \right)^{-1/4} \left(\frac{\Omega_{\text{ALP}}^{\text{VR}}}{0.12} \right)^{1/4} \left(\frac{m_{\text{ULA}}}{10^{-22} \text{ eV}} \right)^{1/2}. \quad (91.34)$$

On non-linear scales the gradient energy leads to the existence of a class of pseudo-solitons known as oscillatons, or axion stars [197].

Cosmological and astrophysical observations are consistent with the CDM model, and departures from it are only allowed on the scales of the smallest observed DM structures with $M \sim 10^{6-8} M_{\odot}$. The CMB power spectrum and galaxy auto-correlation power spectrum limit the ULA mass to $m_{\text{ULA}} > 10^{-24}$ eV from linear theory of structure formation [190, 198]. Analytic models [199] and N -body simulations [200] for non-linear structures show that halo formation is suppressed in ULA models relative to CDM. This leads to constraints on the ULA mass of $m_{\text{ULA}} > 10^{-22}$ eV from observations of high- z galaxies [200, 201], and $m_{\text{ULA}} > 10^{-21}$ eV from the Lyman-alpha forest flux power spectrum [202]. Including the effects of anharmonicities on structure formation with ALPs can weaken these bounds if the misalignment angle $\Theta_i \approx \pi$ [203]. Cosmological simulations that treat gradient energy in the ULA field beyond the N -body approximation have just recently become available [204, 205], and show, among other things, evidence for the formation of axion stars in the centres of ULA halos (various consequences of axion stars are considered in Refs. [206]). These central axion stars have been conjectured to play a role in the apparently cored density profiles of dwarf spheroidal galaxies, and other central galactic regions [204, 207–209]. However, the relationship between the halo mass and the axion star mass [210] leads to problems with this scenario in some galaxies [211–213]. It should be emphasised that many of the conclusions about the role of ULA axion stars in galactic dynamics are based on use of simulation results that do not contain baryons (however, see Ref. [214]), and feedback [215] could be important.

Inside DM halos the axion gradient energy causes coherence on the de Broglie wavelength and fluctuations on the coherence time [204, 216]. These fluctuations can be thought of as short-lived quasiparticles and lead to relaxation processes that can be described statistically [192, 217] (this relaxation processes also leads to the gravitational condensation of axion stars [218]). The typical relaxation time is:

$$t \sim 10^{10} \text{ years} \left(\frac{m_{\text{ULA}}}{10^{-22} \text{ eV}} \right)^3 \left(\frac{v}{100 \text{ km s}^{-1}} \right)^2 \left(\frac{r}{5 \text{ kpc}} \right)^4, \quad (91.35)$$

where v and r are the velocity and radius of the orbit in the host DM halo.

Relaxation processes such as these are not observed in galaxies, though there are some circumstances where they may be desirable [192]. An absence of observed relaxation can be used to set limits on the ULA mass. An absence of Milky Way disk thickening excludes $m_{\text{ULA}} > 0.6 \times 10^{-22}$ eV [219], while stellar streams give the stronger bound $m_{\text{ULA}} > 1.5 \times 10^{-22}$ eV [220]. The survival of the old star cluster in Eridanus II [221] excludes the range of masses 10^{-21} eV $\lesssim m_{\text{ULA}} \lesssim 10^{-19}$ eV [222]. As in the case of ULA axion stars, current constraints from heating do not fully account for the possible role of baryons.

Finally, one should note that the beyond-CDM physics of ULAs (Jeans scale, relaxation, axion star formation) of course also applies to the QCD axion on smaller length scales. This is of particular interest inside axion miniclusters [175, 176, 218, 223].

91.5.2 *Telescope searches*

The two-photon decay is extremely slow for axions with masses in the CDM regime, but could be detectable for eV masses. The signature would be a quasi-monochromatic emission line from galaxies and galaxy clusters. The expected optical line intensity for DFSZ axions is similar to the continuum night emission. An early search in three rich Abell clusters [224] and a recent search in two rich Abell clusters [225] exclude the ‘‘Telescope’’ range in Fig. 91.1. Of course, axions in this mass range would anyway provide an excessive hot DM contribution.

Very low-mass axions in halos produce a weak quasi-monochromatic radio line. Virial velocities in undisrupted dwarf galaxies are very low, and the axion decay line would therefore be extremely narrow. A search with the Haystack radio telescope on three nearby dwarf galaxies provided a limit $|g_{A\gamma\gamma}| < 1.0 \times 10^{-9}$ GeV $^{-1}$ at 96% CL for $298 < m_A < 363$ μeV [226]. However, this combination of m_A and $g_{A\gamma\gamma}$ does not exclude plausible axion models.

A monochromatic signal is also produced in the conversion of DM axions in the background of slowly varying galactic B -fields [227]. The signal is, however, sensitive to magnetic field power on the scale of the axion mass [228]. Present and future radio telescopes appear to be able to probe ALP DM in the mass range $0.1 - 100$ μeV for couplings $g_{A\gamma\gamma} \gtrsim 10^{-13}$ GeV $^{-1}$ [228] – unfortunately not reaching down to the benchmark QCD axion sensitivity.

Resonant conversion of QCD axion DM in neutron star magnetospheres may give a detectable signal from individual neutron stars for axion masses in the μeV range [229]. Furthermore, stimulated ALP decays in high radiation environments may be detectable, by next-generation radio telescopes such as the Square Kilometer Array, down to $g_{A\gamma\gamma} \gtrsim 10^{-11}$ GeV $^{-1}$, for masses between μeV and 0.1 meV [230].

Photon propagation on an ULA DM background can induce birefringence that can be compared with upper limits from the CMB [231] and may also be probed with other sources such as pulsars [232].

91.5.3 *Microwave cavity experiments*

In a big part of the plausible m_A range for CDM, galactic halo axions may be detected by their resonant conversion into a quasi-monochromatic microwave signal in a high-Q electromagnetic cavity permeated by a strong static B field [6, 233, 234]. The cavity frequency is tunable, and the signal is maximized when the frequency is the total axion energy, rest mass plus kinetic energy, of $\nu = (m_A/2\pi) [1 + \mathcal{O}(10^{-6})]$, the width above the rest mass representing the virial distribution in the galaxy. The frequency spectrum may also contain finer structure from axions more recently fallen into the galactic potential and not yet completely virialized [235, 236].

The feasibility of this technique was established in early experiments (RBF and UF) of relatively small sensitive volume, $\mathcal{O}(1)$ liter), with HFET-based amplifiers, setting limits in the range $4.5 < m_A < 16.3$ μeV [237], but lacking by 2–3 orders of magnitude the sensitivity required to detect

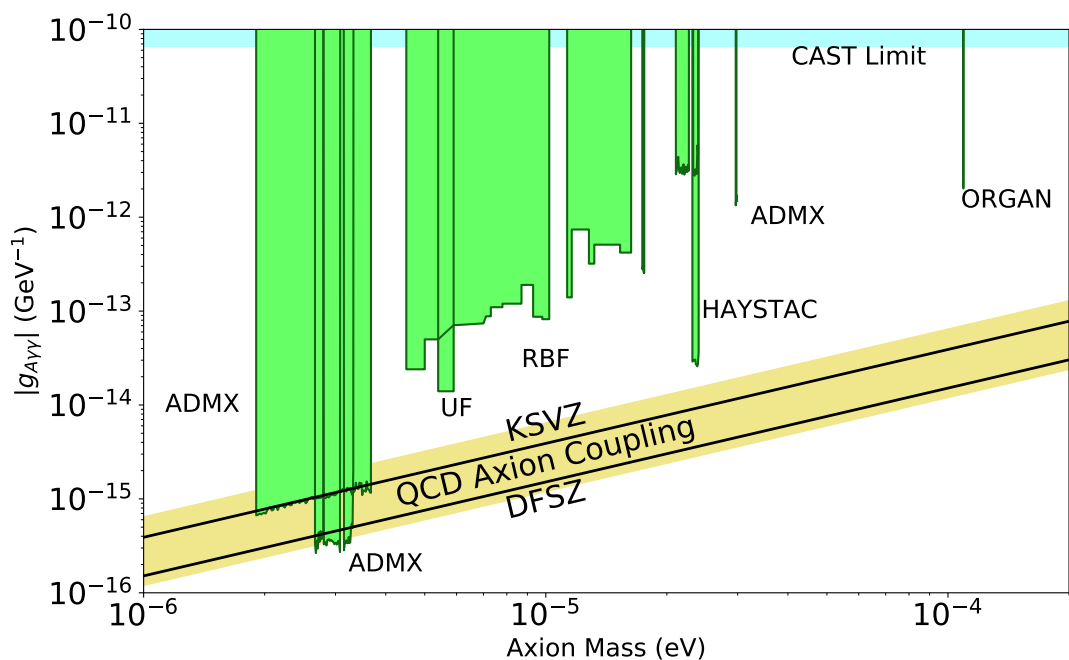


Figure 91.4: Exclusion plot for ALPs as described in the text.

realistic axions, see Fig. 91.4. Later, ADMX ($B \sim 8$ T, $V \sim 200$ liters) has achieved sensitivity to KSVZ axions, assuming they saturate the local DM density and are well virialized, over the mass range $1.9\text{--}3.3$ μeV [238]. Should halo axions have a significant component not yet virialized, ADMX is sensitive to DFSZ axions over the entire mass range [239]. The corresponding 90% CL exclusion regions shown in Fig. 91.4 are normalized to an assumed local CDM density of 7.5×10^{-25} g cm^{-3} (450 MeV cm^{-3}). More recently, the ADMX experiment commissioned an upgrade [240] that replaces the microwave HFET amplifiers by near quantum-limited low-noise dc SQUID microwave amplifiers [241]. It has reached an unprecedented axion DM sensitivity in the mass range between 2.66 and 3.31 μeV [242, 243], down to the DFSZ benchmark axion-photon coupling, see Fig. 91.4. This apparatus is also sensitive to other hypothetical light bosons, such as hidden photons or chameleons, over a limited parameter space [189, 244, 245]. ADMX has also done a testbed experiment to probe higher masses. This experiment lives inside of and operates in tandem with the main ADMX experiment, searches in three widely spaced frequency ranges ($4202\text{--}4249$ MHz, $5086\text{--}5799$ MHz and $7173\text{--}7203$ MHz), uses both the TM_{010} and TM_{020} cavity modes, and demonstrates the successful use of a piezoelectric actuator for cavity tuning [246]. Recently, the HAYSTAC experiment reported on first results from a new microwave cavity search for DM axions with masses above 20 μeV . They exclude axions with two-photon coupling $|g_{A\gamma\gamma}| \gtrsim 2 \times 10^{-14}$ GeV^{-1} over the range 23.15 $\mu\text{eV} < m_A < 24.0$ μeV [247, 248], a factor of 2.7 above the KSVZ benchmark, see Fig. 91.4. Exploiting a Josephson parametric amplifier, this experiment has demonstrated total noise approaching the standard quantum limit for the first time in an axion search. A Rydberg atom single-photon detector [249], like any photon counter, can in principle evade the standard quantum limit for coherent photon detection. The ORGAN experiment is designed to probe axions in the mass range 60 $\mu\text{eV} < m_A < 210$ μeV . In a pathfinding run, it has set the limit $|g_{A\gamma\gamma}| < 2 \times 10^{-12}$ GeV^{-1} at 110 μeV , in a span of 2.5 neV [250]. There are further microwave cavity axion DM experiments recently in operation (CULTASK [251]), under construction (RADES [252]) or proposed (KLASH [253]).

91.5.4 New concepts for axion DM direct detection

Other new concepts for searching for axion DM are also being investigated. An alternative to the microwave cavity technique is based on a novel detector architecture consisting of an open, Fabry-Perot resonator and a series of current-carrying wire planes [254]. The Orpheus detector has demonstrated this new technique, excluding DM ALPs with masses between 68.2 and 76.5 μeV and axion-photon couplings greater than $4 \times 10^{-7} \text{GeV}^{-1}$. This technique may be able to probe DM axions in the mass range from 40 to 700 μeV . Another detector concept exploits the fact that a magnetized mirror would radiate photons in the background of axion DM, which could be collected like in a dish antenna [255]. Searches for hidden photon DM exploiting this technique are already underway [256]. The proposed MADMAX experiment will place a stack of dielectric layers in a magnetic field in order to resonantly enhance the photon signal, aiming a sensitivity to probe the mass range $40 \mu\text{eV} \lesssim m_A \lesssim 200 \mu\text{eV}$ [257, 258]. Optical dielectric haloscopes with single photon signal detection have been proposed to search for axions in the 50 meV – 10 eV mass range [259]. Absorption of axions on molecular transitions can be sensitive to the axion pseudoscalar coupling g_{ANN} to nucleons or the pseudoscalar coupling g_{Aee} to electrons in the 0.5 – 20 eV range [260]. Another proposed axion DM search method sensitive in the 100 μeV mass range is to cool a kilogram-sized sample to mK temperatures and count axion induced atomic transitions using laser techniques [261].

The oscillating galactic DM axion field induces oscillating nuclear electric dipole moments (EDMs) [262],

$$d_N(t) = g_{AN\gamma} \sqrt{2\rho_{\text{ADM}}} \cos(m_A t)/m_A, \quad (91.36)$$

where $g_{AN\gamma}$ is the coupling of the axion to the nucleon EDM operator,

$$\mathcal{L}_A \supset -\frac{i}{2} g_{AN\gamma} A \bar{\Psi}_N \sigma_{\mu\nu} \gamma_5 \Psi_N F^{\mu\nu}. \quad (91.37)$$

For the QCD axion, this coupling is predicted as [263]

$$g_{AN\gamma} = -g_{Ap\gamma} = (3.7 \pm 1.5) \times 10^{-3} \left(\frac{1}{f_A} \right) \frac{1}{\text{GeV}} = (6.5 \pm 2.6) \times 10^{-13} \left(\frac{m_A}{\text{meV}} \right) \frac{1}{\text{GeV}^2} \quad (91.38)$$

and plotted as a yellow diagonal band in Fig. 91.3 (right panel). An analysis of the ratio of spin-precession frequencies of stored ultracold neutrons and ^{199}Hg atoms measured by neutron EDM experiments for an axion-induced oscillating neutron EDM revealed no signal consistent with axion DM, excluding a sizeable region of parameter space in the mass region $10^{-24} \text{eV} \leq m_A \leq 10^{-17} \text{eV}$ [264], which surpass the limits on anomalous energy loss of SN 1987A [262] by more than seven orders of magnitude, but are still a few orders of magnitude above the QCD axion expectations, see Fig. 91.3 (right panel). The oscillating EDMs cause also the precession of nuclear spins in a nucleon spin polarized sample in the presence of an electric field. The resulting transverse magnetization can be searched for by exploiting magnetic-resonance (MR) techniques, which are most sensitive in the range of low oscillation frequencies corresponding to sub-neV axion masses. The aim of the corresponding Cosmic Axion Spin Precession Experiment (CASPER) [265] is to probe axion DM in the anthropic window, $f_A \gtrsim 10^{15} \text{GeV}$ ($m_A \lesssim \text{neV}$), motivated from Grand Unification [266–269]. Sub- μeV ALP masses can also be probed by using the storage ring EDM method proposed in Ref. [270] which exploits a combination of B and E-fields to produce a resonance between the $g-2$ spin precession frequency and the DM ALP field oscillation frequency. This method, however, does not reach the sensitivity to probe the QCD axion prediction for $g_{AN\gamma}$.

In the intermediate mass region, $\text{neV} \lesssim m_A \lesssim 0.1 \mu\text{eV}$, one may exploit a cooled LC circuit and precision magnetometry to search for the oscillating electric current induced by DM axions in a

strong magnetic field [271]. A similar approach is followed by the proposed ABRACADABRA [272] and DM-Radio Pathfinder [273] experiments. Recently, ABRACADABRA-10 cm – a small-scale prototype for a future detector that could be sensitive to the QCD axion – established upper limits on the axion-photon coupling in the mass range 3.1×10^{-10} eV – 8.3×10^{-9} eV [274], which are, however, not competitive yet with other limits in this mass range, see Fig. 91.1.

An eventually non-zero axion electron coupling g_{Aee} will lead to an electron spin precession about the axion DM wind [275]. The QUAX (QUaerere AXions) experiment aims at exploiting MR inside a magnetized material [276]. Because of the higher Larmor frequency of the electron, it is sensitive in the classic window.

91.6 Conclusions

There is a strengthening physics case for very weakly coupled light particles beyond the Standard Model. The elegant solution of the strong CP problem proposed by Peccei and Quinn yields a particularly strong motivation for the axion. In many theoretically appealing ultraviolet completions of the Standard Model axions and ALPs occur automatically. Moreover, they are natural CDM candidates. Perhaps the first hints of their existence have already been seen in the anomalous excessive cooling of stars and the anomalous transparency of the Universe for VHE gamma rays. Interestingly, a significant portion of previously unexplored, but phenomenologically very interesting and theoretically very well motivated axion and ALP parameter space can be tackled in the foreseeable future by a number of terrestrial experiments searching for axion/ALP DM, for solar axions/ALPs, and for light apparently shining through a wall.

References

- [1] R. D. Peccei and H. R. Quinn, Phys. Rev. Lett. **38**, 1440 (1977).
- [2] R. D. Peccei and H. R. Quinn, Phys. Rev. **D16**, 1791 (1977).
- [3] S. Weinberg, Phys. Rev. Lett. **40**, 223 (1978).
- [4] F. Wilczek, Phys. Rev. Lett. **40**, 279 (1978).
- [5] Y. Chikashige, R.N. Mohapatra, and R.D. Peccei, Phys. Lett. **B98**, 265 (1981); G. B. Gelmini and M. Roncadelli, Phys. Lett. **99B**, 411 (1981).
- [6] P. Sikivie, Phys. Rev. Lett. **51**, 1415 (1983) and Erratum *ibid.*, **52**, 695 (1984).
- [7] E. Witten, Phys. Lett. **149B**, 351 (1984).
- [8] J. P. Conlon, JHEP **05**, 078 (2006), [[hep-th/0602233](#)].
- [9] P. Svrcek and E. Witten, JHEP **06**, 051 (2006), [[hep-th/0605206](#)].
- [10] K.-S. Choi *et al.*, Phys. Lett. **B675**, 381 (2009), [[arXiv:0902.3070](#)].
- [11] A. Arvanitaki *et al.*, Phys. Rev. **D81**, 123530 (2010), [[arXiv:0905.4720](#)].
- [12] B. S. Acharya, K. Bobkov and P. Kumar, JHEP **11**, 105 (2010), [[arXiv:1004.5138](#)].
- [13] M. Cicoli, M. Goodsell and A. Ringwald, JHEP **10**, 146 (2012), [[arXiv:1206.0819](#)].
- [14] J. Halverson, C. Long and P. Nath, Phys. Rev. **D96**, 5, 056025 (2017), [[arXiv:1703.07779](#)].
- [15] J. Jaeckel and A. Ringwald, Ann. Rev. Nucl. Part. Sci. **60**, 405 (2010), [[arXiv:1002.0329](#)].
- [16] A. Ringwald, Phys. Dark Univ. **1**, 116 (2012), [[arXiv:1210.5081](#)].
- [17] J. Jaeckel, Frascati Phys. Ser. **56**, 172 (2012), [[arXiv:1303.1821](#)].
- [18] C. A. Baker *et al.*, Phys. Rev. Lett. **97**, 131801 (2006), [[hep-ex/0602020](#)].
- [19] H. Georgi, D. B. Kaplan and L. Randall, Phys. Lett. **169B**, 73 (1986).
- [20] R. J. Crewther, Phys. Lett. **70B**, 349 (1977).
- [21] P. Di Vecchia and G. Veneziano, Nucl. Phys. **B171**, 253 (1980).

- [22] M. Gorghetto and G. Villadoro, *JHEP* **03**, 033 (2019), [[arXiv:1812.01008](#)].
- [23] S. Borsanyi *et al.*, *Nature* **539**, 7627, 69 (2016), [[arXiv:1606.07494](#)].
- [24] J. E. Kim, *Phys. Rev. Lett.* **43**, 103 (1979); M. A. Shifman, A. I. Vainshtein and V. I. Zakharov, *Nucl. Phys.* **B166**, 493 (1980).
- [25] M. Dine, W. Fischler and M. Srednicki, *Phys. Lett.* **104B**, 199 (1981); A. R. Zhitnitsky, *Sov. J. Nucl. Phys.* **31**, 260 (1980), [*Yad. Fiz.*31,497(1980)].
- [26] J. E. Kim and G. Carosi, *Rev. Mod. Phys.* **82**, 557 (2010), [[arXiv:0807.3125](#)].
- [27] G. Grilli di Cortona *et al.*, *JHEP* **01**, 034 (2016), [[arXiv:1511.02867](#)].
- [28] J. E. Kim, *Phys. Rev.* **D58**, 055006 (1998), [[hep-ph/9802220](#)].
- [29] L. Di Luzio, F. Mescia and E. Nardi, *Phys. Rev. Lett.* **118**, 3, 031801 (2017), [[arXiv:1610.07593](#)]; L. Di Luzio, F. Mescia and E. Nardi, *Phys. Rev.* **D96**, 7, 075003 (2017), [[arXiv:1705.05370](#)].
- [30] M. Farina *et al.*, *JHEP* **01**, 095 (2017), [[arXiv:1611.09855](#)].
- [31] P. Agrawal *et al.*, *JHEP* **02**, 006 (2018), [[arXiv:1709.06085](#)].
- [32] G. Raffelt and D. Seckel, *Phys. Rev. Lett.* **60**, 1793 (1988); M. Carena and R. D. Peccei, *Phys. Rev.* **D40**, 652 (1989); K. Choi, K. Kang and J. E. Kim, *Phys. Rev. Lett.* **62**, 849 (1989).
- [33] M. Srednicki, *Nucl. Phys.* **B260**, 689 (1985).
- [34] S. Chang and K. Choi, *Phys. Lett.* **B316**, 51 (1993), [[hep-ph/9306216](#)].
- [35] H. Leutwyler, *Phys. Lett.* **B378**, 313 (1996), [[hep-ph/9602366](#)].
- [36] C. Patrignani *et al.* (Particle Data Group), *Chin. Phys.* **C40**, 10, 100001 (2016).
- [37] D. A. Dicus *et al.*, *Phys. Rev.* **D18**, 1829 (1978).
- [38] G. Raffelt and L. Stodolsky, *Phys. Rev.* **D37**, 1237 (1988).
- [39] A. A. Anselm, *Yad. Fiz.* **42**, 1480 (1985).
- [40] K. van Bibber *et al.*, *Phys. Rev. Lett.* **59**, 759 (1987).
- [41] G. Ruoso *et al.*, *Z. Phys.* **C56**, 505 (1992); R. Cameron *et al.*, *Phys. Rev.* **D47**, 3707 (1993).
- [42] M. Fouche *et al.*, *Phys. Rev.* **D78**, 032013 (2008), [[arXiv:0808.2800](#)].
- [43] P. Pagnat *et al.* (OSQAR), *Phys. Rev.* **D78**, 092003 (2008), [[arXiv:0712.3362](#)].
- [44] A. S. Chou *et al.* (GammeV (T-969)), *Phys. Rev. Lett.* **100**, 080402 (2008), [[arXiv:0710.3783](#)].
- [45] A. Afanasev *et al.*, *Phys. Rev. Lett.* **101**, 120401 (2008), [[arXiv:0806.2631](#)].
- [46] K. Ehret *et al.* (ALPS), *Phys. Lett.* **B689**, 149 (2010), [[arXiv:1004.1313](#)].
- [47] P. Pagnat *et al.* (OSQAR), *Eur. Phys. J.* **C74**, 8, 3027 (2014), [[arXiv:1306.0443](#)].
- [48] R. Ballou *et al.* (OSQAR), *Phys. Rev.* **D92**, 9, 092002 (2015), [[arXiv:1506.08082](#)].
- [49] F. Hoogeveen and T. Ziegenhagen, *Nucl. Phys.* **B358**, 3 (1991).
- [50] P. Sikivie, D. B. Tanner and K. van Bibber, *Phys. Rev. Lett.* **98**, 172002 (2007), [[hep-ph/0701198](#)]; G. Mueller *et al.*, *Phys. Rev.* **D80**, 072004 (2009), [[arXiv:0907.5387](#)].
- [51] R. Baehre *et al.* (ALPS Collab.), *JINST* **1308**, T09001 (2013).
- [52] F. Hoogeveen, *Phys. Lett.* **B288**, 195 (1992).
- [53] J. Jaeckel and A. Ringwald, *Phys. Lett.* **B659**, 509 (2008), [[arXiv:0707.2063](#)].
- [54] F. Caspers, J. Jaeckel and A. Ringwald, *JINST* **4**, P11013 (2009), [[arXiv:0908.0759](#)].

- [55] R. Povey, J. Hartnett and M. Tobar, Phys. Rev. **D82**, 052003 (2010), [[arXiv:1003.0964](#)].
- [56] M. Betz *et al.*, Phys. Rev. **D88**, 7, 075014 (2013), [[arXiv:1310.8098](#)].
- [57] L. Maiani, R. Petronzio and E. Zavattini, Phys. Lett. **B175**, 359 (1986).
- [58] Y. Semertzidis *et al.*, Phys. Rev. Lett. **64**, 2988 (1990).
- [59] E. Zavattini *et al.* (PVLAS), Phys. Rev. Lett. **96**, 110406 (2006), [Erratum: Phys. Rev. Lett. **99**, 129901 (2007)], [[hep-ex/0507107](#)].
- [60] E. Zavattini *et al.* (PVLAS), Phys. Rev. **D77**, 032006 (2008), [[arXiv:0706.3419](#)].
- [61] F. Della Valle *et al.*, Eur. Phys. J. **C76**, 1, 24 (2016), [[arXiv:1510.08052](#)].
- [62] E. Fischbach and C. Talmadge, Nature **356**, 207 (1992).
- [63] J. E. Moody and F. Wilczek, Phys. Rev. **D30**, 130 (1984); A. N. Youdin *et al.*, Phys. Rev. Lett. **77**, 2170 (1996); W.-T. Ni *et al.*, Phys. Rev. Lett. **82**, 2439 (1999); D. F. Phillips *et al.*, Phys. Rev. **D63**, 111101 (2001), [[arXiv:physics/0008230](#)]; B. R. Heckel *et al.*, Phys. Rev. Lett. **97**, 021603 (2006), [[hep-ph/0606218](#)]; S. A. Hoedl *et al.*, Phys. Rev. Lett. **106**, 041801 (2011).
- [64] G. Raffelt, Phys. Rev. **D86**, 015001 (2012), [[arXiv:1205.1776](#)].
- [65] A. Arvanitaki and A. A. Geraci, Phys. Rev. Lett. **113**, 16, 161801 (2014), [[arXiv:1403.1290](#)].
- [66] A. A. Geraci *et al.* (ARIADNE), Springer Proc. Phys. **211**, 151 (2018), [[arXiv:1710.05413](#)].
- [67] M. S. Turner, Phys. Rept. **197**, 67 (1990).
- [68] G. G. Raffelt, Lect. Notes Phys. **741**, 51 (2008), [[51\(2006\)](#)], [[hep-ph/0611350](#)].
- [69] S. Andriamonje *et al.* (CAST), JCAP **0704**, 010 (2007), [[hep-ex/0702006](#)].
- [70] P. Gondolo and G. G. Raffelt, Phys. Rev. **D79**, 107301 (2009), [[arXiv:0807.2926](#)].
- [71] H. Schlattl, A. Weiss and G. Raffelt, Astropart. Phys. **10**, 353 (1999), [[hep-ph/9807476](#)].
- [72] N. Vinyoles *et al.*, JCAP **1510**, 10, 015 (2015), [[arXiv:1501.01639](#)].
- [73] A. Ayala *et al.*, Phys. Rev. Lett. **113**, 19, 191302 (2014), [[arXiv:1406.6053](#)].
- [74] O. Straniero *et al.*, in “Proceedings, 11th Patras Workshop on Axions, WIMPs and WISPs (Axion-WIMP 2015): Zaragoza, Spain, June 22-26, 2015,” 77–81 (2015).
- [75] J. Redondo, JCAP **1312**, 008 (2013), [[arXiv:1310.0823](#)].
- [76] N. Viaux *et al.*, Phys. Rev. Lett. **111**, 231301 (2013), [[arXiv:1311.1669](#)].
- [77] C.-Y. Chen and S. Dawson, Phys. Rev. **D87**, 055016 (2013), [[arXiv:1301.0309](#)].
- [78] G. G. Raffelt, Phys. Lett. **166B**, 402 (1986); S. I. Blinnikov and N. V. Dunina-Barkovskaya, Mon. Not. Roy. Astron. Soc. **266**, 289 (1994).
- [79] M. M. Miller Bertolami *et al.*, JCAP **1410**, 10, 069 (2014), [[arXiv:1406.7712](#)].
- [80] J. Isern *et al.*, Astrophys. J. **682**, L109 (2008), [[arXiv:0806.2807](#)]; J. Isern *et al.*, J. Phys. Conf. Ser. **172**, 012005 (2009), [[arXiv:0812.3043](#)].
- [81] A. Drlica-Wagner *et al.* (LSST Dark Matter Group) (2019), [[arXiv:1902.01055](#)].
- [82] J. Isern *et al.*, Astron. & Astrophys. **512**, A86 (2010); A. H. Corsico *et al.*, Mon. Not. Roy. Astron. Soc. **424**, 2792 (2012), [[arXiv:1205.6180](#)]; A. H. Corsico *et al.*, JCAP **1212**, 010 (2012), [[arXiv:1211.3389](#)].
- [83] A. H. Córscico *et al.* (2019), [[arXiv:1907.00115](#)].
- [84] M. Giannotti *et al.*, JCAP **1710**, 10, 010 (2017), [[arXiv:1708.02111](#)].
- [85] M. Giannotti *et al.*, JCAP **1605**, 05, 057 (2016), [[arXiv:1512.08108](#)].

- [86] G.G. Raffelt, *Stars as Laboratories for Fundamental Physics*, (Univ. of Chicago Press, Chicago, 1996).
- [87] T. Fischer *et al.*, Phys. Rev. **D94**, 8, 085012 (2016), [[arXiv:1605.08780](#)].
- [88] J. H. Chang, R. Essig and S. D. McDermott, JHEP **09**, 051 (2018), [[arXiv:1803.00993](#)].
- [89] P. Carenza *et al.* (2019), [[arXiv:1906.11844](#)].
- [90] J. Engel, D. Seckel and A. C. Hayes, Phys. Rev. Lett. **65**, 960 (1990).
- [91] T. Moroi and H. Murayama, Phys. Lett. **B440**, 69 (1998), [[hep-ph/9804291](#)].
- [92] D. Page *et al.*, Phys. Rev. Lett. **106**, 081101 (2011), [[arXiv:1011.6142](#)].
- [93] P. S. Shternin *et al.*, Mon. Not. Roy. Astron. Soc. **412**, L108 (2011), [[arXiv:1012.0045](#)].
- [94] L. B. Leinson, Phys. Lett. **B741**, 87 (2015), [[arXiv:1411.6833](#)].
- [95] K. Hamaguchi *et al.*, Phys. Rev. **D98**, 10, 103015 (2018), [[arXiv:1806.07151](#)].
- [96] J. Keller and A. Sedrakian, Nucl. Phys. **A897**, 62 (2013), [[arXiv:1205.6940](#)]; A. Sedrakian, Phys. Rev. **D93**, 6, 065044 (2016), [[arXiv:1512.07828](#)].
- [97] L. B. Leinson, JCAP **1408**, 031 (2014), [[arXiv:1405.6873](#)].
- [98] M. V. Beznogov *et al.*, Phys. Rev. **C98**, 3, 035802 (2018), [[arXiv:1806.07991](#)].
- [99] G. G. Raffelt, J. Redondo and N. Viaux Maira, Phys. Rev. **D84**, 103008 (2011), [[arXiv:1110.6397](#)].
- [100] K. van Bibber *et al.*, Phys. Rev. **D39**, 2089 (1989).
- [101] D. M. Lazarus *et al.*, Phys. Rev. Lett. **69**, 2333 (1992).
- [102] S. Moriyama *et al.*, Phys. Lett. **B434**, 147 (1998), [[hep-ex/9805026](#)]; Y. Inoue *et al.*, Phys. Lett. **B536**, 18 (2002), [[arXiv:astro-ph/0204388](#)].
- [103] Y. Inoue *et al.*, Phys. Lett. **B668**, 93 (2008), [[arXiv:0806.2230](#)].
- [104] V. Anastassopoulos *et al.* (CAST), Nature Phys. **13**, 584 (2017), [[arXiv:1705.02290](#)].
- [105] E. Arik *et al.* (CAST), JCAP **0902**, 008 (2009), [[arXiv:0810.4482](#)].
- [106] S. Aune *et al.* (CAST), Phys. Rev. Lett. **107**, 261302 (2011), [[arXiv:1106.3919](#)]; M. Arik *et al.* (CAST), Phys. Rev. Lett. **112**, 9, 091302 (2014), [[arXiv:1307.1985](#)]; M. Arik *et al.* (CAST), Phys. Rev. **D92**, 2, 021101 (2015), [[arXiv:1503.00610](#)].
- [107] E. Armengaud *et al.*, JINST **9**, T05002 (2014), [[arXiv:1401.3233](#)].
- [108] E. Armengaud *et al.* (IAXO), JCAP **1906**, 06, 047 (2019), [[arXiv:1904.09155](#)].
- [109] K. Barth *et al.*, JCAP **1305**, 010 (2013), [[arXiv:1302.6283](#)].
- [110] F. T. Avignone, III *et al.* (SOLAX), Phys. Rev. Lett. **81**, 5068 (1998), [[arXiv:astro-ph/9708008](#)]; S. Cebrian *et al.*, Astropart. Phys. **10**, 397 (1999), [[arXiv:astro-ph/9811359](#)]; A. Morales *et al.* (COSME), Astropart. Phys. **16**, 325 (2002), [[hep-ex/0101037](#)]; R. Bernabei *et al.*, Phys. Lett. **B515**, 6 (2001); Z. Ahmed *et al.* (CDMS), Phys. Rev. Lett. **103**, 141802 (2009), [[arXiv:0902.4693](#)].
- [111] H. Davoudiasl and P. Huber, Phys. Rev. Lett. **97**, 141302 (2006), [[hep-ph/0509293](#)].
- [112] H. S. Hudson *et al.*, ASP Conf. Ser. **455**, 25 (2012), [[arXiv:1201.4607](#)].
- [113] E. Armengaud *et al.*, JCAP **1311**, 067 (2013), [[arXiv:1307.1488](#)]; E. Aprile *et al.* (XENON100), Phys. Rev. **D90**, 6, 062009 (2014), [Erratum: Phys. Rev. **D95**, no.2, 029904 (2017)], [[arXiv:1404.1455](#)].
- [114] D. S. Akerib *et al.* (LUX), Phys. Rev. Lett. **118**, 26, 261301 (2017), [[arXiv:1704.02297](#)].

- [115] J. W. Brockway, E. D. Carlson and G. G. Raffelt, Phys. Lett. **B383**, 439 (1996), [[arXiv:astro-ph/9605197](#)]; J. A. Grifols, E. Masso and R. Toldra, Phys. Rev. Lett. **77**, 2372 (1996), [[arXiv:astro-ph/9606028](#)].
- [116] A. Payez *et al.*, JCAP **1502**, 02, 006 (2015), [[arXiv:1410.3747](#)].
- [117] C. Csaki, N. Kaloper and J. Terning, Phys. Rev. Lett. **88**, 161302 (2002), [[hep-ph/0111311](#)].
- [118] A. Mirizzi, G.G. Raffelt, and P.D. Serpico, Lect. Notes Phys. **741**, 115 (2008).
- [119] R. Gill and J. S. Heyl, Phys. Rev. **D84**, 085001 (2011), [[arXiv:1105.2083](#)].
- [120] D. Horns *et al.*, Phys. Rev. **D85**, 085021 (2012), [[arXiv:1203.2184](#)].
- [121] A. Payez, J. R. Cudell and D. Hutsemekers, JCAP **1207**, 041 (2012), [[arXiv:1204.6187](#)].
- [122] A. Dominguez, M. A. Sanchez-Conde and F. Prada, JCAP **1111**, 020 (2011), [[arXiv:1106.1860](#)].
- [123] W. Essey and A. Kusenko, Astrophys. J. **751**, L11 (2012), [[arXiv:1111.0815](#)].
- [124] D. Horns and M. Meyer, JCAP **1202**, 033 (2012), [[arXiv:1201.4711](#)].
- [125] G. I. Rubtsov and S. V. Troitsky, JETP Lett. **100**, 6, 355 (2014), [Pisma Zh. Eksp. Teor. Fiz.100,no.6,397(2014)], [[arXiv:1406.0239](#)].
- [126] K. Kohri and H. Kodama, Phys. Rev. **D96**, 5, 051701 (2017), [[arXiv:1704.05189](#)].
- [127] D. A. Sanchez, S. Fegan and B. Giebels, Astron. Astrophys. **554**, A75 (2013), [[arXiv:1303.5923](#)].
- [128] J. Biteau and D. A. Williams, Astrophys. J. **812**, 1, 60 (2015), [[arXiv:1502.04166](#)].
- [129] A. Domínguez and M. Ajello, Astrophys. J. **813**, 2, L34 (2015), [[arXiv:1510.07913](#)].
- [130] A. De Angelis, G. Galanti and M. Roncadelli, Phys. Rev. **D84**, 105030 (2011), [Erratum: Phys. Rev.D87,no.10,109903(2013)], [[arXiv:1106.1132](#)]; M. Simet, D. Hooper and P. D. Serpico, Phys. Rev. **D77**, 063001 (2008), [[arXiv:0712.2825](#)]; M. A. Sanchez-Conde *et al.*, Phys. Rev. **D79**, 123511 (2009), [[arXiv:0905.3270](#)].
- [131] M. Meyer, D. Horns and M. Raue, Phys. Rev. **D87**, 3, 035027 (2013), [[arXiv:1302.1208](#)].
- [132] A. Abramowski *et al.* (H.E.S.S.), Phys. Rev. **D88**, 10, 102003 (2013), [[arXiv:1311.3148](#)].
- [133] M. Ajello *et al.* (Fermi-LAT), Phys. Rev. Lett. **116**, 16, 161101 (2016), [[arXiv:1603.06978](#)].
- [134] C. Zhang *et al.*, Phys. Rev. **D97**, 6, 063009 (2018), [[arXiv:1802.08420](#)].
- [135] Z.-Q. Xia *et al.*, Phys. Rev. **D97**, 6, 063003 (2018), [[arXiv:1801.01646](#)].
- [136] J. Majumdar, F. Calore and D. Horns, JCAP **1804**, 04, 048 (2018), [[arXiv:1801.08813](#)].
- [137] S. S. Wilks, Annals Math. Statist. **9**, 1, 60 (1938).
- [138] D. Wouters and P. Brun, Astrophys. J. **772**, 44 (2013), [[arXiv:1304.0989](#)].
- [139] M. Berg *et al.*, Astrophys. J. **847**, 2, 101 (2017), [[arXiv:1605.01043](#)].
- [140] M. C. D. Marsh *et al.*, JCAP **1712**, 12, 036 (2017), [[arXiv:1703.07354](#)].
- [141] J. P. Conlon *et al.*, JCAP **1707**, 07, 005 (2017), [[arXiv:1704.05256](#)].
- [142] L. Chen and J. P. Conlon, Mon. Not. Roy. Astron. Soc. **479**, 2, 2243 (2018), [[arXiv:1712.08313](#)].
- [143] C. S. Reynolds *et al.* (2019), [[arXiv:1907.05475](#)].
- [144] A. Arvanitaki and S. Dubovsky, Phys. Rev. **D83**, 044026 (2011), [[arXiv:1004.3558](#)].
- [145] A. Arvanitaki, M. Baryakhtar and X. Huang, Phys. Rev. **D91**, 8, 084011 (2015), [[arXiv:1411.2263](#)].

- [146] A. Arvanitaki *et al.*, Phys. Rev. **D95**, 4, 043001 (2017), [[arXiv:1604.03958](#)].
- [147] K. K. Y. Ng *et al.* (2019), [[arXiv:1908.02312](#)].
- [148] M. S. Turner, Phys. Rev. Lett. **59**, 2489 (1987), [Erratum: Phys. Rev. Lett.60,1101(1988)]; E. Masso, F. Rota and G. Zsembinszki, Phys. Rev. **D66**, 023004 (2002), [[hep-ph/0203221](#)]; P. Graf and F. D. Steffen, Phys. Rev. **D83**, 075011 (2011), [[arXiv:1008.4528](#)].
- [149] S. Hannestad *et al.*, JCAP **1008**, 001 (2010), [[arXiv:1004.0695](#)]; M. Archidiacono *et al.*, JCAP **1310**, 020 (2013), [[arXiv:1307.0615](#)]; E. Di Valentino *et al.*, Phys. Lett. **B752**, 182 (2016), [[arXiv:1507.08665](#)].
- [150] M. Archidiacono *et al.*, JCAP **1505**, 05, 050 (2015), [[arXiv:1502.03325](#)].
- [151] E. Masso and R. Toldra, Phys. Rev. **D55**, 7967 (1997), [[hep-ph/9702275](#)]; D. Cadamuro and J. Redondo, JCAP **1202**, 032 (2012), [[arXiv:1110.2895](#)].
- [152] J. Preskill, M. B. Wise and F. Wilczek, Phys. Lett. **B120**, 127 (1983); L. F. Abbott and P. Sikivie, Phys. Lett. **B120**, 133 (1983); M. Dine and W. Fischler, Phys. Lett. **B120**, 137 (1983).
- [153] K. J. Bae, J.-H. Huh and J. E. Kim, JCAP **0809**, 005 (2008), [[arXiv:0806.0497](#)].
- [154] O. Wantz and E. P. S. Shellard, Phys. Rev. **D82**, 123508 (2010), [[arXiv:0910.1066](#)].
- [155] G. Ballesteros *et al.*, JCAP **1708**, 08, 001 (2017), [[arXiv:1610.01639](#)].
- [156] M. Tegmark *et al.*, Phys. Rev. **D73**, 023505 (2006), [[arXiv:astro-ph/0511774](#)].
- [157] A. D. Linde, Phys. Lett. **158B**, 375 (1985).
- [158] D. Seckel and M. S. Turner, Phys. Rev. **D32**, 3178 (1985).
- [159] M. Beltran, J. Garcia-Bellido and J. Lesgourgues, Phys. Rev. **D75**, 103507 (2007), [[hep-ph/0606107](#)].
- [160] M. P. Hertzberg, M. Tegmark and F. Wilczek, Phys. Rev. **D78**, 083507 (2008), [[arXiv:0807.1726](#)].
- [161] J. Hamann *et al.*, JCAP **0906**, 022 (2009), [[arXiv:0904.0647](#)].
- [162] P. A. R. Ade *et al.* (Planck), Astron. Astrophys. **571**, A22 (2014), [[arXiv:1303.5082](#)].
- [163] P. A. R. Ade *et al.* (Planck), Astron. Astrophys. **594**, A20 (2016), [[arXiv:1502.02114](#)].
- [164] S. Chang, C. Hagmann and P. Sikivie, Phys. Rev. **D59**, 023505 (1999), [[hep-ph/9807374](#)].
- [165] C. Hagmann, S. Chang and P. Sikivie, Phys. Rev. **D63**, 125018 (2001), [[hep-ph/0012361](#)].
- [166] T. Hiramatsu *et al.*, Phys. Rev. **D83**, 123531 (2011), [[arXiv:1012.5502](#)].
- [167] T. Hiramatsu *et al.*, Phys. Rev. **D85**, 105020 (2012), [Erratum: Phys. Rev.D86,089902(2012)], [[arXiv:1202.5851](#)].
- [168] M. Kawasaki, K. Saikawa and T. Sekiguchi, Phys. Rev. **D91**, 6, 065014 (2015), [[arXiv:1412.0789](#)].
- [169] V. B. Klaer and G. D. Moore, JCAP **1711**, 11, 049 (2017), [[arXiv:1708.07521](#)].
- [170] M. Gorghetto, E. Hardy and G. Villadoro, JHEP **07**, 151 (2018), [[arXiv:1806.04677](#)].
- [171] M. Buschmann, J. W. Foster and B. R. Safdi (2019), [[arXiv:1906.00967](#)].
- [172] M. Hindmarsh *et al.* (2019), [[arXiv:1908.03522](#)].
- [173] A. Ringwald and K. Saikawa, Phys. Rev. **D93**, 8, 085031 (2016), [Addendum: Phys. Rev.D94,no.4,049908(2016)], [[arXiv:1512.06436](#)].
- [174] T. Hiramatsu *et al.*, JCAP **1301**, 001 (2013), [[arXiv:1207.3166](#)].

- [175] C. J. Hogan and M. J. Rees, Phys. Lett. **B205**, 228 (1988).
- [176] E. W. Kolb and I. I. Tkachev, Phys. Rev. Lett. **71**, 3051 (1993), [[hep-ph/9303313](#)].
- [177] K. M. Zurek, C. J. Hogan and T. R. Quinn, Phys. Rev. **D75**, 043511 (2007), [[arXiv:astro-ph/0607341](#)].
- [178] A. Vaquero, J. Redondo and J. Stadler (2018), [[JCAP1904,no.04,012\(2019\)](#)], [[arXiv:1809.09241](#)].
- [179] E. W. Kolb and I. I. Tkachev, Astrophys. J. **460**, L25 (1996), [[arXiv:astro-ph/9510043](#)].
- [180] M. Fairbairn, D. J. E. Marsh and J. Quevillon, Phys. Rev. Lett. **119**, 2, 021101 (2017), [[arXiv:1701.04787](#)].
- [181] A. Katz *et al.*, JCAP **1812**, 005 (2018), [[arXiv:1807.11495](#)].
- [182] E. Berkowitz, M. I. Buchoff and E. Rinaldi, Phys. Rev. **D92**, 3, 034507 (2015), [[arXiv:1505.07455](#)].
- [183] S. Borsanyi *et al.*, Phys. Lett. **B752**, 175 (2016), [[arXiv:1508.06917](#)].
- [184] R. Kitano and N. Yamada, JHEP **10**, 136 (2015), [[arXiv:1506.00370](#)].
- [185] P. Petreczky, H.-P. Schadler and S. Sharma, Phys. Lett. **B762**, 498 (2016), [[arXiv:1606.03145](#)].
- [186] Y. Taniguchi *et al.*, Phys. Rev. **D95**, 5, 054502 (2017), [[arXiv:1611.02411](#)].
- [187] M. Dine *et al.*, Phys. Rev. **D96**, 9, 095001 (2017), [[arXiv:1705.00676](#)].
- [188] R. D. Pisarski and L. G. Yaffe, Phys. Lett. **97B**, 110 (1980).
- [189] P. Arias *et al.*, JCAP **1206**, 013 (2012), [[arXiv:1201.5902](#)].
- [190] R. Hlozek *et al.*, Phys. Rev. **D91**, 10, 103512 (2015), [[arXiv:1410.2896](#)].
- [191] D. J. E. Marsh, Phys. Rept. **643**, 1 (2016), [[arXiv:1510.07633](#)].
- [192] L. Hui *et al.*, Phys. Rev. **D95**, 4, 043541 (2017), [[arXiv:1610.08297](#)].
- [193] A. G. Dias *et al.*, JHEP **06**, 037 (2014), [[arXiv:1403.5760](#)]; J. E. Kim and D. J. E. Marsh, Phys. Rev. **D93**, 2, 025027 (2016), [[arXiv:1510.01701](#)].
- [194] H. Davoudiasl and C. W. Murphy, Phys. Rev. Lett. **118**, 14, 141801 (2017), [[arXiv:1701.01136](#)].
- [195] M. Khlopov, B. A. Malomed and I. B. Zeldovich, Mon. Not. Roy. Astron. Soc. **215**, 575 (1985).
- [196] W. Hu, R. Barkana and A. Gruzinov, Phys. Rev. Lett. **85**, 1158 (2000), [[arXiv:astro-ph/0003365](#)]; L. Amendola and R. Barbieri, Phys. Lett. **B642**, 192 (2006), [[hep-ph/0509257](#)]; D. J. E. Marsh and P. G. Ferreira, Phys. Rev. **D82**, 103528 (2010), [[arXiv:1009.3501](#)].
- [197] E. Seidel and W. M. Suen, Phys. Rev. Lett. **66**, 1659 (1991).
- [198] R. Hlozek, D. J. E. Marsh and D. Grin, Mon. Not. Roy. Astron. Soc. **476**, 3, 3063 (2018), [[arXiv:1708.05681](#)].
- [199] D. J. E. Marsh and J. Silk, Mon. Not. Roy. Astron. Soc. **437**, 3, 2652 (2014), [[arXiv:1307.1705](#)].
- [200] H.-Y. Schive *et al.*, Astrophys. J. **818**, 1, 89 (2016), [[arXiv:1508.04621](#)].
- [201] B. Bozek *et al.*, Mon. Not. Roy. Astron. Soc. **450**, 1, 209 (2015), [[arXiv:1409.3544](#)]; P. S. Corasaniti *et al.*, Phys. Rev. **D95**, 8, 083512 (2017), [[arXiv:1611.05892](#)].
- [202] E. Armengaud *et al.*, Mon. Not. Roy. Astron. Soc. **471**, 4, 4606 (2017), [[arXiv:1703.09126](#)]; V. Iršič *et al.*, Phys. Rev. Lett. **119**, 3, 031302 (2017), [[arXiv:1703.04683](#)]; T. Kobayashi *et al.*, Phys. Rev. **D96**, 12, 123514 (2017), [[arXiv:1708.00015](#)].

- [203] H.-Y. Schive and T. Chiueh, *Mon. Not. Roy. Astron. Soc.* **473**, 1, L36 (2018), [[arXiv:1706.03723](#)].
- [204] H.-Y. Schive, T. Chiueh and T. Broadhurst, *Nature Phys.* **10**, 496 (2014), [[arXiv:1406.6586](#)].
- [205] B. Schwabe, J. C. Niemeyer and J. F. Engels, *Phys. Rev.* **D94**, 4, 043513 (2016), [[arXiv:1606.05151](#)]; J. Veltmaat and J. C. Niemeyer, *Phys. Rev.* **D94**, 12, 123523 (2016), [[arXiv:1608.00802](#)]; P. Mocz *et al.*, *Mon. Not. Roy. Astron. Soc.* **471**, 4, 4559 (2017), [[arXiv:1705.05845](#)].
- [206] D. G. Levkov, A. G. Panin and I. I. Tkachev, *Phys. Rev. Lett.* **118**, 011301 (2017); T. Helfer *et al.*, *JCAP* **1703**, 03, 055 (2017), [[arXiv:1609.04724](#)].
- [207] D. J. E. Marsh and A.-R. Pop, *Mon. Not. Roy. Astron. Soc.* **451**, 3, 2479 (2015), [[arXiv:1502.03456](#)]; S.-R. Chen, H.-Y. Schive and T. Chiueh, *Mon. Not. Roy. Astron. Soc.* **468**, 2, 1338 (2017), [[arXiv:1606.09030](#)]; A. X. González-Morales *et al.*, *Mon. Not. Roy. Astron. Soc.* **472**, 2, 1346 (2017), [[arXiv:1609.05856](#)].
- [208] I. De Martino *et al.* (2018), [[arXiv:1807.08153](#)].
- [209] T. Broadhurst *et al.* (2019), [[arXiv:1902.10488](#)].
- [210] H.-Y. Schive *et al.*, *Phys. Rev. Lett.* **113**, 26, 261302 (2014), [[arXiv:1407.7762](#)].
- [211] V. H. Robles, J. S. Bullock and M. Boylan-Kolchin, *Mon. Not. Roy. Astron. Soc.* **483**, 1, 289 (2019), [[arXiv:1807.06018](#)].
- [212] V. Desjacques and A. Nusser (2019), [[arXiv:1905.03450](#)].
- [213] M. Safarzadeh and D. N. Spergel (2019), [[arXiv:1906.11848](#)].
- [214] J. H. H. Chan *et al.*, *Mon. Not. R. Astron. Soc* **478**, 2686 (2018), [[arXiv:1712.01947](#)].
- [215] A. Pontzen and F. Governato, *Nature* **506**, 171 (2014), [[arXiv:1402.1764](#)].
- [216] J. Veltmaat, J. C. Niemeyer and B. Schwabe, *Phys. Rev.* **D98**, 4, 043509 (2018), [[arXiv:1804.09647](#)].
- [217] B. Bar-Or, J.-B. Fouvry and S. Tremaine, *Astrophys. J.* **871**, 1, 28 (2019), [[arXiv:1809.07673](#)].
- [218] D. G. Levkov, A. G. Panin and I. I. Tkachev, *Phys. Rev. Lett.* **121**, 15, 151301 (2018), [[arXiv:1804.05857](#)].
- [219] B. V. Church, P. Mocz and J. P. Ostriker, *Mon. Not. R. Astron. Soc* **485**, 2861 (2019), [[arXiv:1809.04744](#)].
- [220] N. C. Amorisco and A. Loeb (2018), [[arXiv:1808.00464](#)].
- [221] T. S. Li *et al.* (DES), *Astrophys. J.* **838**, 1, 8 (2017), [[arXiv:1611.05052](#)].
- [222] D. J. E. Marsh and J. C. Niemeyer, *Phys. Rev. Lett.* **123**, 5, 051103 (2019), [[arXiv:1810.08543](#)].
- [223] B. Eggemeier and J. C. Niemeyer (2019), [[arXiv:1906.01348](#)].
- [224] M. A. Bershadsky, M. T. Ressler and M. S. Turner, *Phys. Rev. Lett.* **66**, 1398 (1991); M. T. Ressler, *Phys. Rev.* **D44**, 3001 (1991).
- [225] D. Grin *et al.*, *Phys. Rev.* **D75**, 105018 (2007), [[arXiv:astro-ph/0611502](#)].
- [226] B. D. Blout *et al.*, *Astrophys. J.* **546**, 825 (2001), [[arXiv:astro-ph/0006310](#)].
- [227] K. Kelley and P. J. Quinn, *Astrophys. J.* **845**, 1, L4 (2017), [[arXiv:1708.01399](#)].
- [228] G. Sigl, *Phys. Rev.* **D96**, 10, 103014 (2017), [[arXiv:1708.08908](#)].
- [229] A. Hook *et al.*, *Phys. Rev. Lett.* **121**, 24, 241102 (2018), [[arXiv:1804.03145](#)].
- [230] A. Caputo *et al.*, *JCAP* **1903**, 03, 027 (2019), [[arXiv:1811.08436](#)].

- [231] M. A. Fedderke, P. W. Graham and S. Rajendran, Phys. Rev. **D100**, 1, 015040 (2019), [[arXiv:1903.02666](#)].
- [232] T. Liu, G. Smoot and Y. Zhao (2019), [[arXiv:1901.10981](#)].
- [233] P. Sikivie, Phys. Rev. **D32**, 2988 (1985), [Erratum: Phys. Rev. **D36**, 974 (1987)].
- [234] R. Bradley *et al.*, Rev. Mod. Phys. **75**, 777 (2003).
- [235] P. Sikivie and J. R. Ipser, Phys. Lett. **B291**, 288 (1992).
- [236] P. Sikivie, I. I. Tkachev and Y. Wang, Phys. Rev. Lett. **75**, 2911 (1995), [[arXiv:astro-ph/9504052](#)].
- [237] S. De Panfilis *et al.*, Phys. Rev. Lett. **59**, 839 (1987); W. Wuensch *et al.*, Phys. Rev. **D40**, 3153 (1989); C. Hagmann *et al.*, Phys. Rev. **D42**, 1297 (1990).
- [238] S. J. Asztalos *et al.* (ADMX), Phys. Rev. **D69**, 011101 (2004), [[arXiv:astro-ph/0310042](#)].
- [239] L. Duffy *et al.*, Phys. Rev. Lett. **95**, 091304 (2005), [[arXiv:astro-ph/0505237](#)]; J. Hoskins *et al.*, Phys. Rev. **D84**, 121302 (2011), [[arXiv:1109.4128](#)].
- [240] S. J. Asztalos *et al.* (ADMX), Phys. Rev. Lett. **104**, 041301 (2010), [[arXiv:0910.5914](#)].
- [241] S. J. Asztalos *et al.* (ADMX), Nucl. Instrum. Meth. **A656**, 39 (2011), [[arXiv:1105.4203](#)].
- [242] N. Du *et al.* (ADMX), Phys. Rev. Lett. **120**, 15, 151301 (2018), [[arXiv:1804.05750](#)].
- [243] T. Braine *et al.* (ADMX) (2019), [[arXiv:1910.08638](#)].
- [244] G. Rybka *et al.* (ADMX), Phys. Rev. Lett. **105**, 051801 (2010), [[arXiv:1004.5160](#)].
- [245] A. Wagner *et al.* (ADMX), Phys. Rev. Lett. **105**, 171801 (2010), [[arXiv:1007.3766](#)].
- [246] C. Boutan *et al.* (ADMX), Phys. Rev. Lett. **121**, 26, 261302 (2018), [[arXiv:1901.00920](#)].
- [247] B. M. Brubaker *et al.*, Phys. Rev. Lett. **118**, 6, 061302 (2017), [[arXiv:1610.02580](#)].
- [248] L. Zhong *et al.* (HAYSTAC), Phys. Rev. **D97**, 9, 092001 (2018), [[arXiv:1803.03690](#)].
- [249] I. Ogawa, S. Matsuki and K. Yamamoto, Phys. Rev. **D53**, R1740 (1996).
- [250] B. T. McAllister *et al.*, Phys. Dark Univ. **18**, 67 (2017), [[arXiv:1706.00209](#)].
- [251] W. Chung, PoS **CORFU2015**, 047 (2016).
- [252] A. A. Melcon *et al.* (RADES), JCAP **1805**, 05, 040 (2018), [[arXiv:1803.01243](#)].
- [253] D. Alesini *et al.* (KLASH) (2017), [[arXiv:1707.06010](#)].
- [254] G. Rybka *et al.*, Phys. Rev. **D91**, 1, 011701 (2015), [[arXiv:1403.3121](#)].
- [255] D. Horns *et al.*, JCAP **1304**, 016 (2013), [[arXiv:1212.2970](#)].
- [256] J. Suzuki *et al.*, JCAP **1509**, 09, 042 (2015), [[arXiv:1504.00118](#)].
- [257] A. Caldwell *et al.* (MADMAX Working Group), Phys. Rev. Lett. **118**, 9, 091801 (2017), [[arXiv:1611.05865](#)].
- [258] P. Brun *et al.* (MADMAX), Eur. Phys. J. **C79**, 3, 186 (2019), [[arXiv:1901.07401](#)].
- [259] M. Baryakhtar, J. Huang and R. Lasenby, Phys. Rev. **D98**, 3, 035006 (2018), [[arXiv:1803.11455](#)].
- [260] A. Arvanitaki, S. Dimopoulos and K. Van Tilburg, Phys. Rev. **X8**, 4, 041001 (2018), [[arXiv:1709.05354](#)].
- [261] P. Sikivie, Phys. Rev. Lett. **113**, 20, 201301 (2014), [[arXiv:1409.2806](#)].
- [262] P. W. Graham and S. Rajendran, Phys. Rev. **D88**, 035023 (2013), [[arXiv:1306.6088](#)].
- [263] M. Pospelov and A. Ritz, Nucl. Phys. **B573**, 177 (2000), [[hep-ph/9908508](#)].

- [264] C. Abel *et al.*, Phys. Rev. **X7**, 4, 041034 (2017), [[arXiv:1708.06367](#)].
- [265] D. Budker *et al.*, Phys. Rev. **X4**, 2, 021030 (2014), [[arXiv:1306.6089](#)].
- [266] M. B. Wise, H. Georgi and S. L. Glashow, Phys. Rev. Lett. **47**, 402 (1981).
- [267] A. Ernst, A. Ringwald and C. Tamarit, JHEP **02**, 103 (2018), [[arXiv:1801.04906](#)].
- [268] L. Di Luzio, A. Ringwald and C. Tamarit, Phys. Rev. **D98**, 9, 095011 (2018), [[arXiv:1807.09769](#)].
- [269] P. Fileviez Perez, C. Murgui and A. D. Plascencia (2019), [[arXiv:1908.01772](#)].
- [270] S. P. Chang *et al.*, Phys. Rev. **D99**, 8, 083002 (2019), [[arXiv:1710.05271](#)].
- [271] P. Sikivie, N. Sullivan, and D. B. Tanner, Phys. Rev. Lett. **112**, 131301 (2014).
- [272] Y. Kahn, B. R. Safdi and J. Thaler, Phys. Rev. Lett. **117**, 14, 141801 (2016), [[arXiv:1602.01086](#)].
- [273] M. Silva-Feaver *et al.*, IEEE Trans. Appl. Supercond. **27**, 4, 1400204 (2017), [[arXiv:1610.09344](#)].
- [274] J. L. Ouellet *et al.* (ABRACADABRA), Phys. Rev. Lett. **122**, 12, 121802 (2019), [[arXiv:1810.12257](#)].
- [275] L. Krauss *et al.*, Phys. Rev. Lett. **55**, 1797 (1985).
- [276] R. Barbieri *et al.*, Phys. Dark Univ. **15**, 135 (2017).